Evaluation of the Bubble Spectrometer Performance in Space-Like Neutron Fields

by

Talon James Montague

A thesis submitted to the
School of Graduate and Postdoctoral Studies in partial
fulfillment of the requirements for the degree of

Master of Applied Science in Nuclear Engineering

Faculty of Energy Systems and Nuclear Science

University of Ontario Institute of Technology (Ontario Tech University)

Oshawa, Ontario, Canada

February 2021

THESIS EXAMINATION INFORMATION

Submitted by: **Talon Montague**

Master of Applied Science in Nuclear Engineering

Thesis title: Evaluation of the Bubble Spectrometer Performance in Space-Like Neutron Fields

An oral defense of this thesis took place on November 27, 2020, in front of the following examining committee:

Examining Committee:

Chair of Examining Committee	Dr. Jennifer McKellar
Research Supervisor	Dr. Rachid Machrafi
Examining Committee Member	Dr. Igor Pioro
Examining Committee Member	Dr. Kirk Atkinson
Thesis Examiner	Dr. Filippo Genco

The above committee determined that the thesis is acceptable in form and content and that a satisfactory knowledge of the field covered by the thesis was demonstrated by the candidate during an oral examination. A signed copy of the Certificate of Approval is available from the School of Graduate and Postdoctoral Studies.

ABSTRACT

The Space Bubble Detector Spectrometer (SBDS) consists of six bubble detectors each with a different neutron energy threshold. To characterize the spectrometer in a space-like neutron field, a series of experiments were conducted with high-energy neutrons from 6.0×10^5 eV to 7.50×10^8 eV at the Los Alamos National Laboratory. The analysis of the obtained data provided a calibration factor to adjust the neutron sensitivity, to high-energy neutrons of the SBDS, based on its response function matrix. The results suggest that the SBDS underestimates the ambient dose equivalent in a space-like neutron field by a factor of approximately 1.55. Consequently, the readings of the spectrometer should be adjusted when used in a space radiation environment.

This thesis is dedicated to studying the SBDS in a space-like neutron spectrum. It outlines a part of the results of international ground testing experimental sessions of the space instrumentation supported by the Canadian Space Agency.

Keywords: Spectrometer; Space Bubble Detector; International Space Station.

AUTHOR'S DECLARATION

I hereby declare that this thesis consists of original work of which I have authored. This is a true copy of the thesis, including any required final revisions, as accepted by my examiners.

I authorize the University of Ontario Institute of Technology (Ontario Tech University) to lend this thesis to other institutions or individuals for the purpose of scholarly research. I further authorize the University of Ontario Institute of Technology (Ontario Tech University) to reproduce this thesis by photocopying or by other means, in total or in part, at the request of other institutions or individuals for the purpose of scholarly research. I understand that my thesis will be made electronically available to the public.

_____ Talon Montague

STATEMENT OF CONTRIBUTIONS

The work described in Chapter 3 was performed at the Los Alamos Neutron Science Center (LANSCE) in New Mexico, USA, by Dr. Rachid Machrafi. I was responsible for recording the bubble detector counts using the bubble reader BDR-III.

I was also responsible for the analysis of the experimental data collected in different experiments. I solely performed the analysis and calculations presented in Chapter 4.

I hereby certify that I am the sole author of this thesis and that no part of this thesis has been published or submitted for publication. I have used standard referencing practices to acknowledge ideas, research techniques, or other materials that belong to others. Furthermore, I hereby certify that I am the sole source of the creative works and/or inventive knowledge described in this thesis.

ACKNOWLEDGEMENTS

I would like to thank my supervisor, Dr. Rachid Machrafi who encouraged me and supported me through all my research work.

THESIS CONTRIBUTIONS TO THE FIELD

We have made a notable contribution to the field of neutron dose measurements in low earth orbit. The Bubble detector spectrometer calibrated with mono-energetic neutrons up to 300×10^6 eV has been irradiated in a high-energy neutron field to determine an appropriate adjustment factor for measurements onboard the International Space Station or other space vehicles.

TABLE OF CONTENTS

LIST OF FIGURES

LIST OF TABLES

LIST OF NOMENCLATURE

Acronyms

BBND	Bonner Ball Neutron Detector
BDR-III	Bubble Detector Reader III
BDS	Bubble Detector Spectrometer
BTI	Bubble Technology Industries
CERN	European Organization for Nuclear Research
GCR	Galactic Cosmic Rays
ICE House	Irradiation of Chips and Electronics
ICRP	International Commission on Radiological Protection
ISO	International Organization for Standardization
ISS	International Space Station
JEM	Japanese Experiment Module
LANSCE	Los Alamos Neutron Science Center
LOE	Low Earth Orbit
NASA	National Aeronautics and Space Administration

PBD	Personal Bubble Detector
SBDS	Space Bubble Detector Spectrometer
SI	International System
TEPC	Tissue Equivalent Proportional Counter
TOF	Time-of-Flight
UOIT	University of Ontario Institute of Technology
USA	United States of America

Symbols and Units

Am	Americium
Be	Beryllium
BF	Boron Trifluoride
C	Carbon
Cf	Californium
CF	Conversion Factor
$Cf_k(E_n)$	Fluence to dose conversion coefficient
D	Absorbed Dose

d	Distance
E	Energy
eV	Electron Volt
$F_k(E_n)$	Neutron fluence at energy bin number k [cm^{-2}]
Gy	Gray [J/kg]
H	Equivalent Dose [Sv]
Hz	Hertz
J	Joules
keV	Kilo-Electron Volt [10^3 eV]
kg	Kilogram
L	Litre
Li	Lithium
m	Meter
MeV	Mega Electron Volt [10^6 eV]
ml	Millilitre [10^{-3} L]
mrem	Milli-rem [10^{-3} rem]

mSv	Milli-Sieverts [10^{-3} Sv]
N	Number of Neutrons
pSv	Pico-Sieverts [10^{-12} Sv]
Q	Quality Factor
R	Standardized response [mrem]
rem	Roentgen Equivalent Man
Sv	Sieverts, unit of equivalent dose
T	Titanium
t	Time
v	Velocity
μm	Micrometer (micron) [10^{-6} m]
σ	Detector Average Response over a specific energy interval [cm^2]
ϕ	Flux [cm^{-2} s^{-1}]

Chapter 1. Introduction

Personal Space Bubble Detector (PSBD) and Bubble Detector Spectrometer (BDS) are Canadian made radiation devices. The technology is a well-established terrestrial neutron radiation measurement instrument. They have also been used in space and space flight applications since 1989 [1]. A significant portion of the radiation dose received by crew members aboard the ISS is from protons and neutrons because of the large flux of these particles in that environment [2]. Neutrons specifically are difficult to accurately measure because they are uncharged particles that interact with matter in complex ways of which the probability of occurrence depends on the incident energy and the target nuclei structure [3]. Due to the complex nature of the space radiation field experienced on the International Space Station (ISS), researchers have also considered the heavy charged particle contribution to the readings of the bubble detector in the space environment [4].

Besides the bubble detector, there have been other technologies used in space for radiation measurements. One of those detection devices was the Bonner Ball Neutron Detector (BBND), which was used in an experiment on the ISS as a part of NASA's (National Aeronautics and Space Administration) Human Research Facility project to evaluate the neutron radiation environment in the energy range of thermal up to 1.5×10^7 eV [5]. This detector is a series of six sensors that has a proportional counter for thermal neutrons covered by a neutron moderator.

There have also been tissue equivalent proportional counters (TEPC) used to determine the neutron spectrum aboard the ISS. The TEPC detector can measure the absorbed dose

directly because the detector setup is designed to be equivalent to human tissue. Uk-Won Nam et al in 2013 conducted experiments with TEPC aboard the ISS [6].

The Space Bubble Detector (SBD) is a bubble detector that produces bubbles in the emulsion gel when exposed to different radiation particles. A digital reader is then used to create an image of the detector and count the number of bubbles [7]. The number of bubbles is directly proportional to the number of interactions that occur in the gel, which in turn allows for the number of bubbles generated to provide a dose measurement. The Space Bubble Detector Spectrometer (SBDS) is also used for neutron radiation measurements in space. The spectrometer is a set of six bubble detectors, each with a different neutron energy threshold for bubble formation. After the bubble detector reader images all six detectors and evaluates the bubble counts, a response matrix is used to determine the neutron spectrum [8].

Since the establishment of the ISS, many experiments in low Earth orbit (LEO) have used this technology. Recent experiments were conducted as part of the Matroshka-R and Radi-N projects. These studies were carried out over several ISS missions to contribute to the following areas: a better understanding of the neutron radiation fields the crew members are exposed to, their corresponding neutron portion of total equivalent dose, and study the neutron field behind different shielding materials [9] [10] [11]. Neutron radiation makes up from ~30% to 50% of the equivalent dose astronauts receive in LEO [9].

In the ISS orbit, factors such as the solar activity cycle and orbital parameters play a role in the radiation environment. With this complexity, there have been studies in space for dose measured by bubble detectors, but very few have investigated SBDS. SBDS have

been used during the Radi-N experiment onboard the ISS. In this experiment, similar to the work presented in this thesis, a set of six detectors was used with different energy thresholds to measure the neutron energy spectrum and neutron dose equivalent [10]. Since the neutron sensitivity of the SBDS is calibrated using mono-energetic neutrons on Earth up to 300 MeV, a calibration factor must be used to get a more accurate neutron dose equivalent in an extended neutron spectrum similar to the one encountered aboard on the ISS.

This thesis outlines the results of the experimental sessions conducted with SBDS as a part of the detector ground testing supported by the Canadian Space Agency. Results compare the neutron dose measurement in space-like neutron spectra from the spallation source at the Los Alamos Neutron Science Center (LANSCE), measured with a Time-Of-Flight (TOF) Spectrometer, to the neutron dose measured with SBDS. This comparison allows for the development of a calibration factor when using SBDS in LOE on the ISS.

The thesis consists of an introduction, three chapters, a conclusion, future work, and the thesis ends with a list of references and appendices. The introduction gives a brief overview of bubble detector technology, its use, and states the current status of its use in space research. Chapter one is dedicated to a description of neutron interactions, neutron sources, and presents the terrestrial and space research with bubble detectors and dosimeters. Chapter two describes the methodology used in this work which consists of the description of the Los Alamos neutron facility, the space bubble spectrometer, and the bubble reader. This chapter also provides the calibration method of the bubble spectrometer and details the unfolding technique to derive the dose value from the readings of the spectrometer. Chapter three discusses the results obtained in a series of experiments where the bubble

spectrometer was exposed to high-energy neutrons from 6.0×10^{5} eV to 7.50×10^{8} eV at the Los Alamos neutron facility. The conclusion summarizes the main findings and gives some insights into future work and the use of the bubble spectrometer in a space environment.

Chapter 2. Background

2.1 Neutron Sources

Being aware of where neutrons can originate from is a key component in understanding neutron dosimetry. In most cases, neutrons are the result of various reactions occurring in the nucleus of an atom. If there is enough energy deposited in an atom, a neutron can be ejected. These reactions can be naturally occurring or artificially created. In general, there are no naturally occurring neutron emitters of significance [12]. More likely, an unstable nucleus with extra neutrons will transform a neutron into a proton rather than emit a neutron (beta minus decay).

Since naturally occurring neutron emitters are virtually not available, they must be artificially created by reactions that produce neutrons. These neutron resultant reactions include:

a) Alpha-neutron reaction sources

b) Gamma-neutron reaction sources

c) Fission reaction sources

2.1.1 Alpha-Neutron Reaction Sources

This type of neutron source is commonly used in the nuclear industry and is normally found in different research facilities. As the name suggests, neutrons from this type of source are created from a light nucleus exposed to an alpha particle emitter. The alpha particle then interacts with a low Z material (low number of protons, such as ^{9}Be), resulting in a neutron being emitted with a daughter particle and energy in the form of gamma [13] [14]. For this

reaction to occur, the alpha energy must be sufficient enough to pass through the Coulomb barrier and exceed the threshold energy requirement (neutron energy separation). The energies of the resulting neutrons are dependent on the nucleus energy levels, and the alpha particle emitter. The maximum energy occurs when the nucleus is left in the ground state and the neutron travels in the same direction as the emitted alpha particle [14].

One example of this neutron source type is the Americium-Beryllium (AmBe) source. Americium and Beryllium are some of the most common emitters and converters respectively, and the combination of these two is typically used in a laboratory setting. The long half-life makes this neutron source practical for research and training purposes [15].

2.1.2 Gamma-Neutron Reaction Sources

When a gamma-ray of sufficient energy, to overcome the neutron binding energy, comes into contact with a nucleus, there is a chance that a neutron is ejected and an isotope is created [14]. These types of neutron sources are best known as photoneutrons. As the gamma energy increases, the photoneutron cross-section increases.

When it comes to neutron shielding problems, this form of neutron emission is of low concern. There are only a few light elements with a large enough photoneutron cross-section for there to be any significance. A few of those elements are ^{2}H, ^{6}Li, and ^{9}Be [14].

2.1.3 Fission Reaction Sources

Fission reaction is another source of neutrons. This reaction can occur spontaneously or after a nucleus has absorbed an incoming neutron. Once a fission event occurs, fission products and neutrons are released. The majority of these neutrons are created almost immediately. Secondary neutrons, or delayed neutrons, are released as a result of the fission

products decaying up to minutes after the fission event [14]. A neutron source is required to start these fission reactions, however once started can exponentially multiply the number of neutrons being created due to more than one neutron resulting from each fission event.

Spontaneous fission occurs in atoms with a heavy nucleus. These unstable heavy radionuclides can decay through alpha particle emission, or in some cases spontaneous fission. There are some naturally occurring radionuclides where the spontaneous fission probability is large enough to produce a neutron source [16]. The most commonly used spontaneous fission source is ^{252}Cf. It decays about 97% of the time through alpha particle emission, and the other 3% by spontaneous fission.

2.2 Neutron Interactions

Onboard the ISS, or any scenario where a person might obtain neutron dose, it is important to understand how neutrons interact with matter. The most important mode of interaction in bubble detector measurements is the scattering process.

Neutrons are uncharged particles that are not affected by the Coulomb repulsion, making them effective at penetrating materials. As a result of having no charge, neutrons will virtually only interact with a nucleus, either through scattering or absorption reactions.

2.2.1 Neutron Scattering

The two types of scattering interactions are elastic and inelastic. For elastic scattering, the neutron scatters off of a nucleus, altering its direction and losing some of its energy. The energy transfer to the nucleus is not sufficient enough to change it to an excited state and is therefore left in a ground state [17]. Inelastic scattering, however, is when there is

sufficient energy transfer from the neutron to the nucleus to induce an excited state. Since the nucleus is in an excited state, it then decays through the emission of gamma rays [17].

This neutron interaction is the mechanism in which fast neutrons are thermalized, giving them a higher probability to be absorbed.

2.2.2 Neutron Radiative Capture

In this interaction, the incoming neutron is absorbed by the nucleus and as a result, the nucleus is elevated to an excited state. The energy is then released in the form of gamma rays to bring the nucleus back to its ground state.

2.2.3 Neutron Fission

This type of reaction was explained in Section 2.1.3, however, should be listed as both a neutron source and a neutron interaction mechanism. Many different heavy nuclei, when absorbing a neutron, enter an excited state. In this excited state, they split apart into smaller particles (fission fragments) and usually release two to three neutrons. The point at which this event will occur is called the critical energy of fission [14].

Fission is of small concern, however, Michael F. L'Annunziata explains in his textbook that ^{10}B can undergo fission, splitting into ^{4}H and ^{7}Li [15]. These particles have a very short range of travel and therefore can be shielded sufficiently with most material [15].

2.3 Neutron Detection with Bubble Detectors

Bubble detectors are commonly used as a neutron dosimeter. The detectors have many benefits in the nuclear industry and are the only personal dosimeters that meet the International Committee of Radiation Protection 60 (ICRP) recommendations for a neutron

dosimeter [16]. These devices generate real-time monitoring output of neutron dose, have a high sensitivity, are portable, and also provide a visual reading of dose from the bubbles created.

There are different kinds of bubble detectors, but this thesis will focus solely on the space bubble detectors manufactured by Bubble Technology Industries (BTI) as these devices are the ones used onboard the International Space Station for neutron radiation measurement.

Bubble detectors are a passive form of dosimeter that produces bubbles when exposed to radiation. Superheated droplets of a low boiling point liquid are suspended in viscoelastic emulsion gel. The superheated state of the droplets vaporizes upon interaction with ionizing radiation if the amount of energy deposited is sufficient within a certain critical length [18]. The ionizing radiation then produces bubbles in the gel, as long as the minimum energy for bubble nucleation is met. This results in bubble detectors having a specific radiation response. The number of bubbles is directly proportional to the number of interactions that occur in the gel, which in turn allows for the number of bubbles generated to provide a dose measurement.

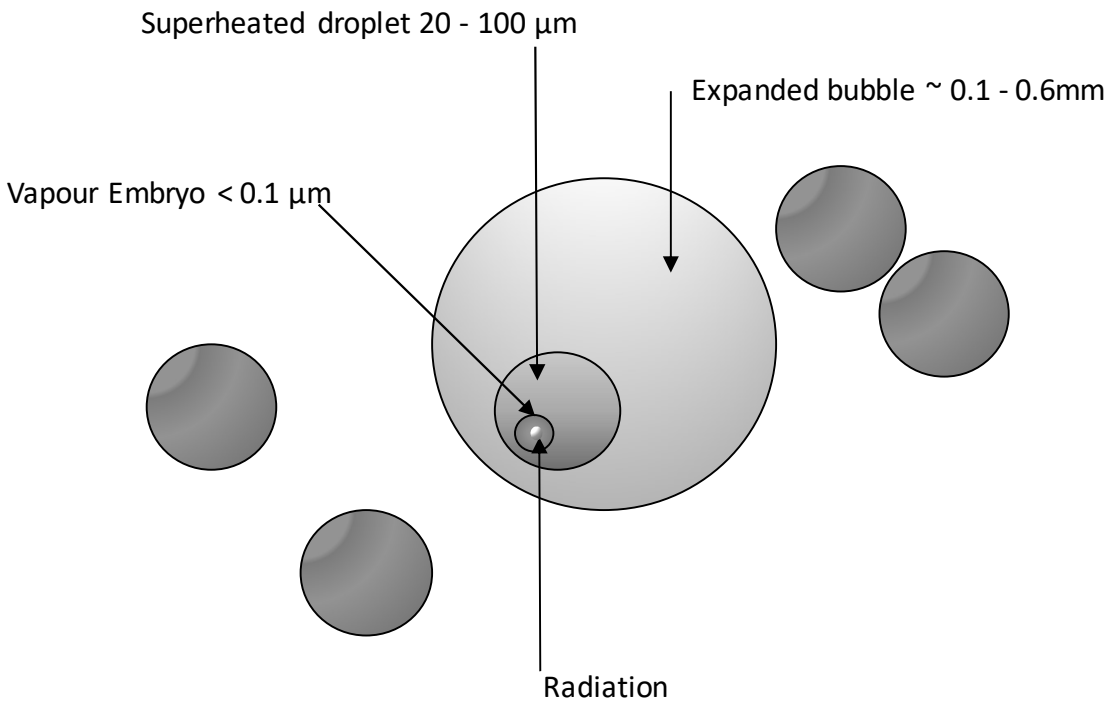

Figure 1: Bubble Formation in Superheated Emulsions

For the BDS made by BTI, the detectors are 0.08 m in length and 0.016 m in diameter [19]. There is 0.01 liter of gel encapsulated in a plastic tube with a metal pistol on one end. This metal piston keeps the gel under pressure. When a measurement is to be taken, the piston is released to a lower pressure to allow the formation of bubbles when irradiated. The space bubble detector is shown in Figure 2.

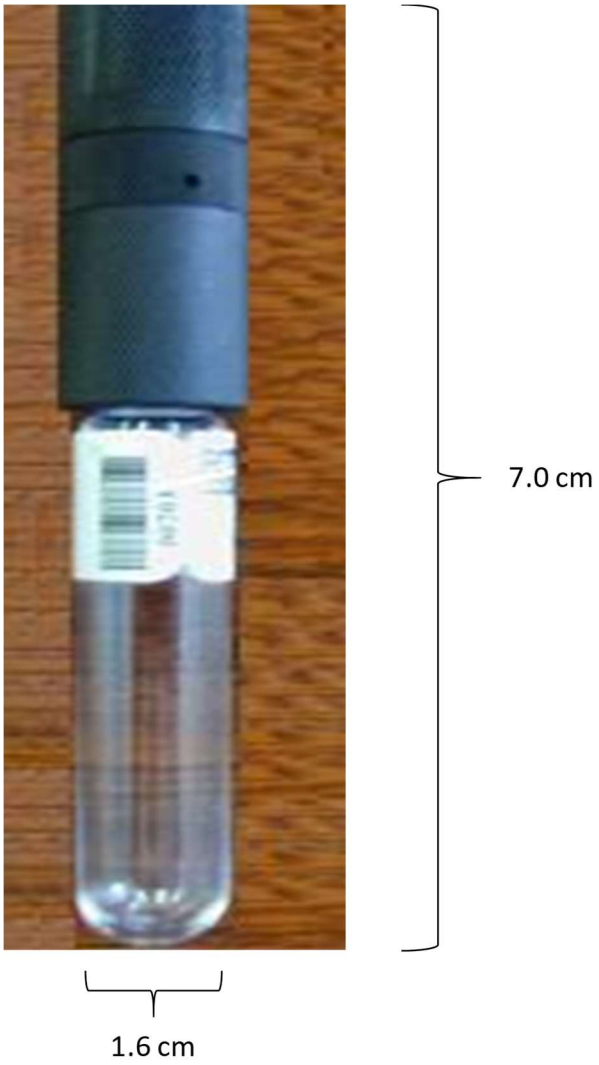

Figure 2: Space Bubble Detector

Once the bubble detector has been irradiated, the Bubble Detector Reader III (BDR-III) made by BTI is used to count and analyze the droplets created. Once the user enters the serial number and the sensitivity of the SBD, the device then automatically counts the number of bubbles formed and calculates the neutron dose [20]. The bubble detector reader BDR-III is presented in Figure 3.

Figure 3: BDR-III Bubble Detector Reader III from BTI [20]

2.4 Neutron Dosimetry Concepts

2.4.1 Neutron Absorbed Dose

Absorbed dose is a quantification of energy that is imparted to matter and is the simplest form of dose measure. This amount of energy is then divided by the mass of the body, given in units of J/kg, also known as rad or Gray (Gy). The Gray unit has been adopted as the unit of measure in the International System (SI) of units. Where 1 J/kg equals 1 Gy, which also equals 100 rad.

2.4.3 Neutron Equivalent Dose

Absorbed dose in its simplicity measures the energy imparted over mass. However, that is not always a sufficient indication of the actual effects imparted on the mass itself. For

example, comparing the same absorbed doses, alpha particles do more damage than protons, and protons do more damage than beta particles. The relationship is that the damage increases as the distance over which the energy is imparted decreases [21]. Other factors affect the damage done by one ionizing particle, such as the type material being irradiated and the length of time the dose is obtained.

To obtain the equivalent dose, the damage a particle does must be factored in. Thus, the absorbed dose is multiplied by a quality factor, which expresses the effectiveness of a given particle to produce damage. The equivalent dose is measured in rem, or the SI unit Sieverts (Sv), and is expressed using the following equation [21]:

$$H = D \times Q$$

Where:

H is the dose equivalent,

D is the absorbed dose,

Q is the quality factor.

Studies have built on this concept to define the Effective Dose which describes the whole-body effective dose of a radiation exposure event, applying considerations of different organs and their sensitivity to radiation [7].

Determining the effective dose received by all organs in the body is not a practical quantity to measure since it can be difficult to know the exposure to each specific organ. For radiation protection, the Ambient Dose Equivalent is more suitable. This measurement is

the total equivalent dose (with the quality factors associated) for the whole body from a radiation field penetrating 0.01 m into a 0.3 m sphere [22]. This calculation provides an estimate for the whole body dose, without requiring complex mathematical models or detailed information on specific exposures to internal organs.

2.4.4 Neutron Fluence to Dose Conversion Factor

A spacecraft experiences complex neutron radiation fields with large variations in particle types and energies. Rather than calculating the ambient equivalent dose received, the neutron fluence multiplied by fluence to dose conversion factors is used to determine the equivalent dose. ICRP has developed neutron fluence to dose conversion factors to calculate the total equivalent dose in a radiation field with a known fluence.

The equivalent dose is integrated over all neutron energies in the radiation field. It is denoted as:

$$H = \int_0^\infty \phi(E) \times CF(E) dE$$

Where:

$\phi(E)$ is the neutron flux at energy E,

CF is the conversion factor at each energy level [23].

The fluence to dose conversion factors over neutron energies from 10 eV to 7.5×10^8 eV used in this study are from ICRP 74 [24] as shown in the figure below.

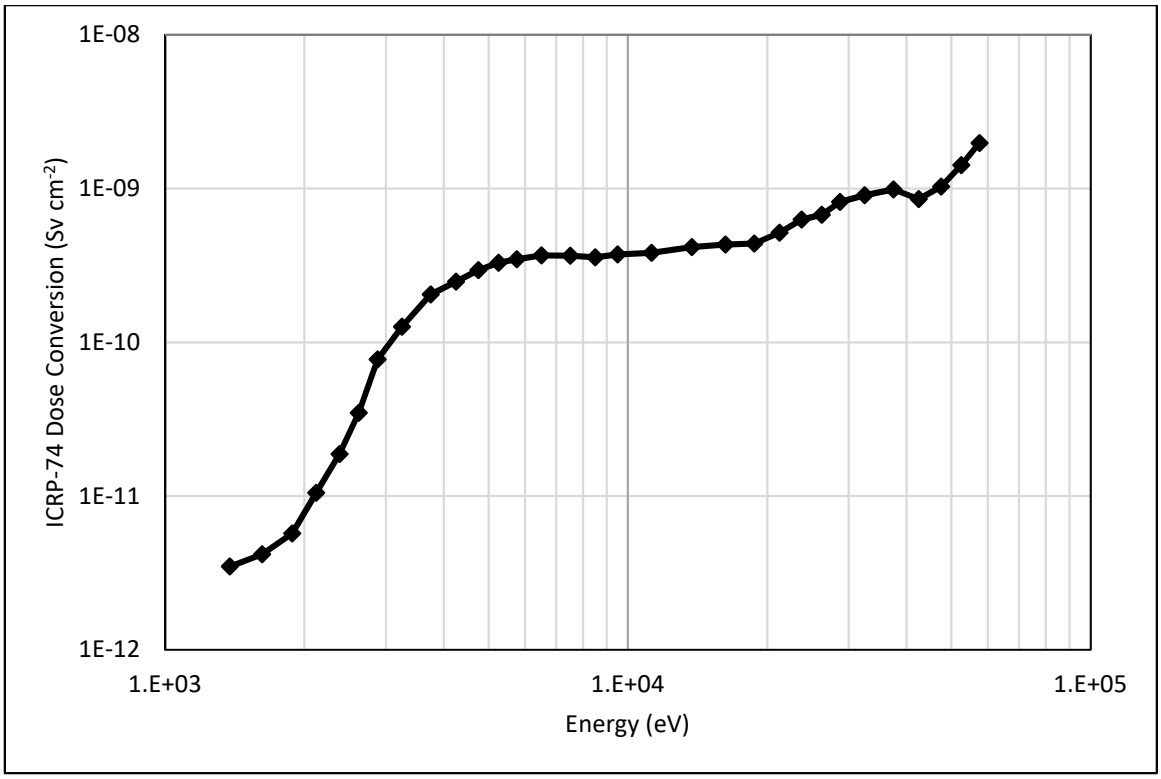

Figure 4: ICRP74 Conversion Factor [24]

2.5 Galactic Cosmic Rays

Since the majority of neutron dose measurements have taken place in LEO, the work conducted in this study focuses on similar neutron spectra. In this scenario, one of the main contributors to neutron production is Galactic Cosmic Rays (GCRs). These GCRs are protons, alpha particles, and heavy charged particles that mostly originate from beyond our solar system. On average, they are made up of 89% protons, 10% helium nuclei, and 1% other heavy elements [25]. These particles travel near the speed of light coming from exploding stars, giving them large amounts of energy [26]. The flux is not constant but varies due to the Sun's solar activity and the Earth's magnetic field. Figure 5 illustrates GCRs in our solar system.

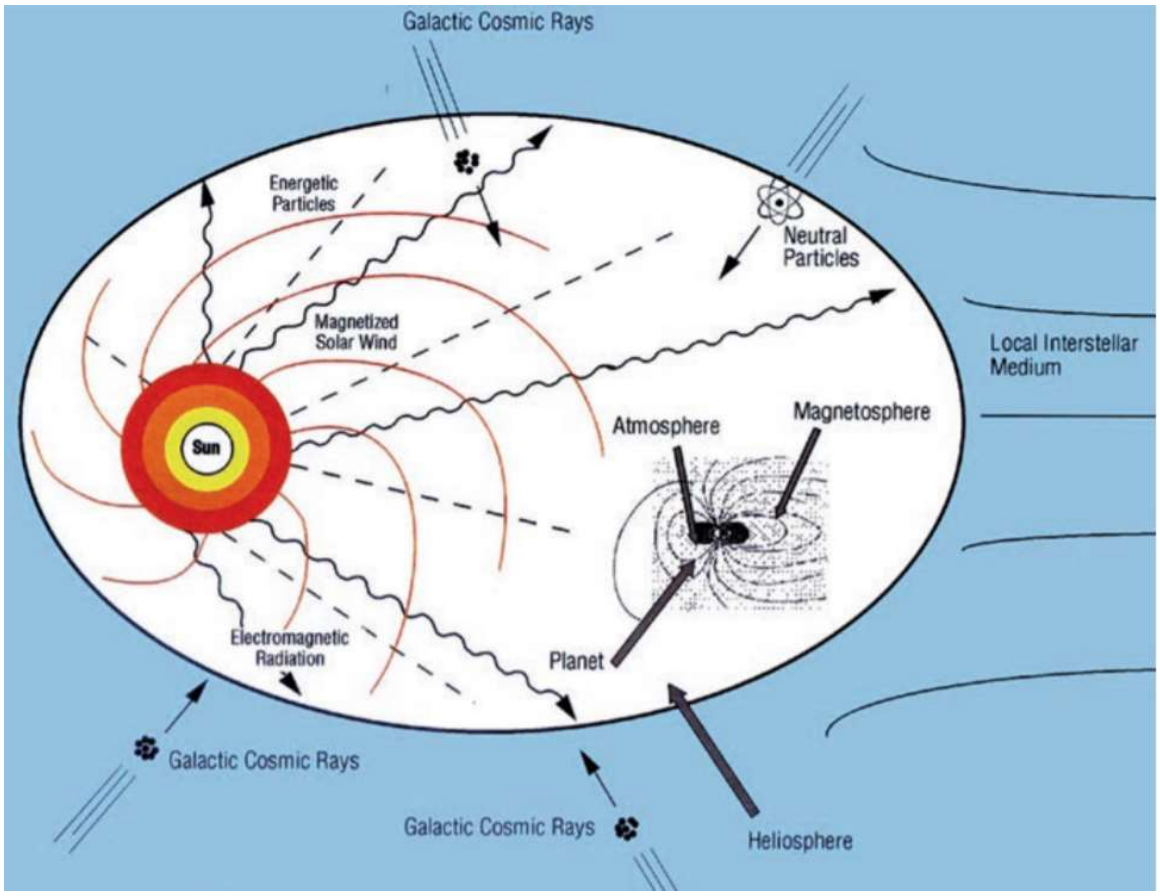

Figure 5: Galactic Cosmic Rays [26]

2.5.1 Neutron Environment in Space

The ionizing radiation environment encountered in space is complex and with higher intensity compared to that on Earth. This includes photons, protons, heavy charged particles, alpha particles, and neutrons. In this study, the neutron environment in space will be the focus.

A major concern for space travel and exploration is the damage caused by neutron radiation to spacecraft components and crew members. There are virtually no neutrons in the primary space radiation environment [27]. The neutrons experienced aboard the ISS are produced

when GCRs interact with the structural components of spacecraft as a result of different nuclear reactions such as nuclear spallation [28]. These secondary neutrons can have high energies of up to several hundred MeV, resulting in a high dose equivalent contribution.

2.5.2 Studies of Neutron Fields in Space

Besides the bubble detectors, the neutron radiation field aboard the international space station has been evaluated using different detection methods and detectors.

The BBND experiment was conducted in the US Laboratory Module of the ISS as part of NASA's Human Research Facility project to evaluate the neutron radiation environment in the energy range of thermal up to 1.5×10^7 eV [5]. This experiment was conducted over eight months in 2001 from March to November. The neutron energy spectrum measured as part of the experiment was compared with the model spectrum that was predicted. The BBND consists of a ^{3}He spherical proportional counter sensitive to thermal neutrons covered by six layers of neutron moderators. One moderator is made of polyethylene spheres of varying thicknesses, and the second moderator is gadolinium which eliminates thermal neutrons. The experiment concluded showed that the measurements and the Monte Carlo model are in good agreement for energies above 10^7 eV, however, the predictive model had a lower flux for energies lower than 10^7 eV [5]. This was attributed to the difference in shielding.

There have also been TEPC detectors used to determine the neutron spectrum onboard the ISS. These types of detectors measure the absorbed dose directly because TEPC uses a material equivalent to human tissue. A material needs to be selected that has the same scattering and absorption characteristics that a human body would regarding radiation

interaction. Uk-Won Nam et al. in 2013 developed a TEPC detector for radiation monitoring onboard the ISS and evaluated the characteristics of the detector [6]. The developed detector was comprised of tissue-equivalent material A-150, with a mass ratio of 10.2% hydrogen, 77.6% carbon, and 5.2% oxygen to mirror the human body. The tissue-equivalent gas used had a mass ratio of C_3H_8 (55%) + CO_2 (39.6%) + N_2 (5.5%) for the internal detection gas. The result of this design was used for future radiation monitoring aboard the ISS [6]. To calibrate the dose readings, the instrument was irradiated using a ^{252}Cf standard neutron source at the Korean Research Institute of Standards and Science. The design was created to have the capability of measuring the equivalent dose on the human body in real-time.

TEPC measurements in space have taken place well before the design created by Uk-Won Nam et al. Measurements using this type of detector were performed during the Antares mission in 1992 inside the Russian MIR Space Station [29]. Like all TEPC designs, this one was comprised of a cylinder with low-pressure gas equivalent to biological tissue. Measurements during this experiment were carried out over three years continuously. During that period, the Antares mission lasted 12 days, with the total dose equivalent being measured at 0.012 Sv for that time. Conclusive ties were made in this research between increased dose received on the space station and increased solar activity. Due to the nature of TEPC technology, it was also concluded that these real-time dose equivalent measuring devices are an adequate active detector for long-term operations in space [29].

Figure 6 shows the results of bubble detector measures on the ISS from November 2009 to July 2012. The ISS altitude is also shown in that figure for reference [30]. There was a significant increase in the altitude from 3.5×10^5 m to 4.25×10^6 m. It would be expected

that the measured dose would increase during the period of increased altitude, however, the bubble detectors did not show any increase in readings. Figure 7 shows the comparison of absorbed dose measurements between the DB-8 detectors and TEPC [30]. These measurements were taken at the same time as the bubble detectors, so both figures side by side show a comparison between all three detector types. DB-8 and TEPC results showed an increase in the absorbed dose with the increase in altitude of the ISS. It was noted that the difference in measurements between the three technologies could be attributed to DB-8 being sensitive only to heavy charged particles, while TEPC detectors measure the absorbed dose from all sources including neutrons. Increased altitude may have resulted in a decrease in neutrons in the radiation field, which would correspond to the decrease in bubble counts from the bubble detectors.

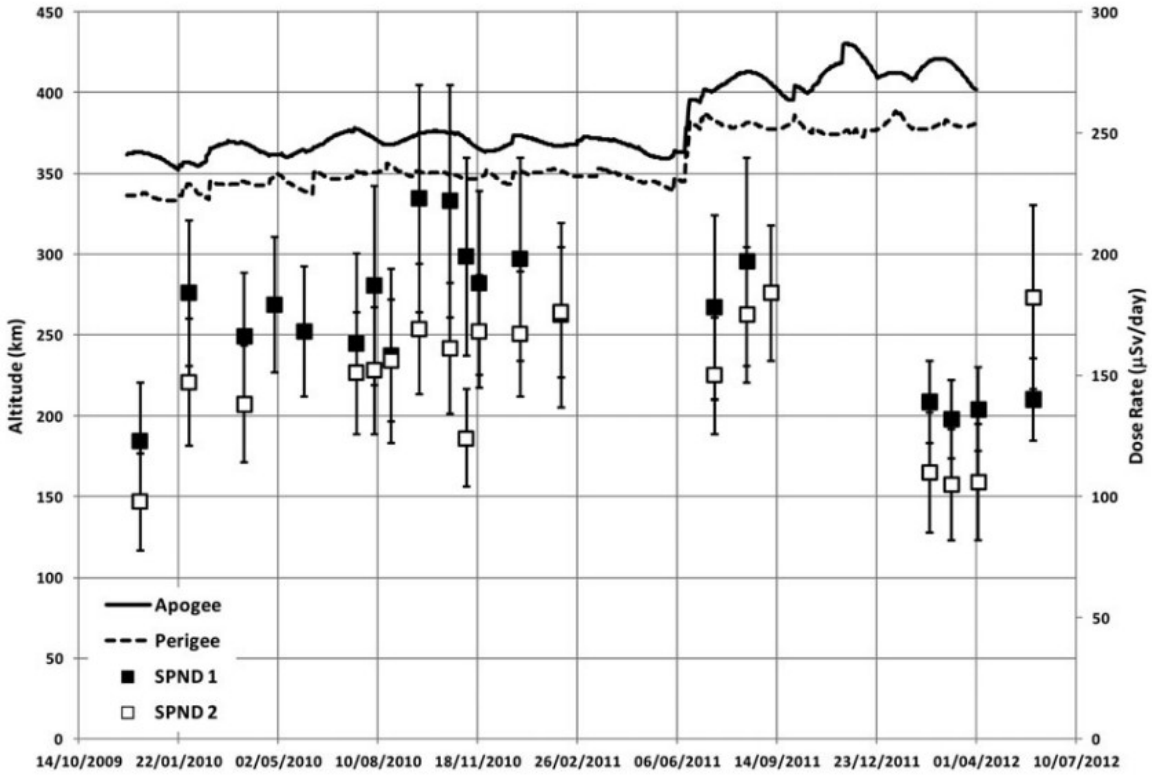

Figure 6: Dose Rates Measured using SPND [30]

(Figure reproduced with permission from Oxford University Press)

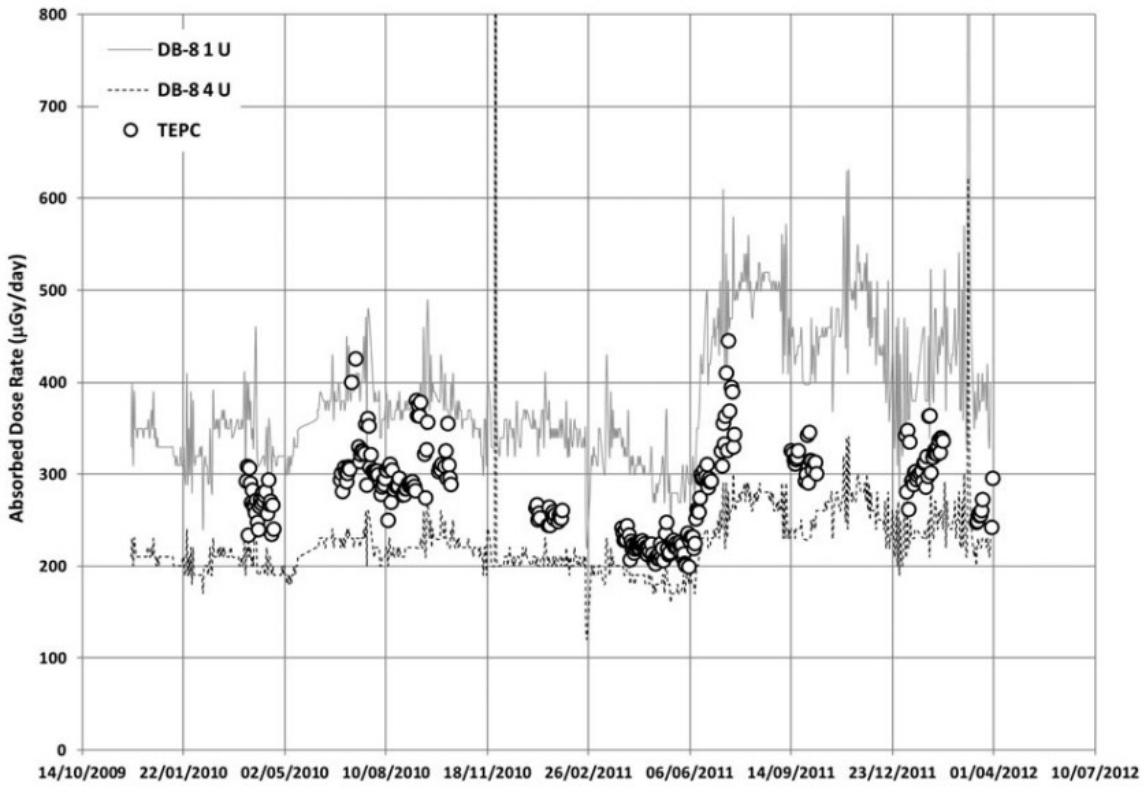

Figure 7: Comparison of Space Absorbed Dose Rates between DB-8 and TEPC [30]

(Figure reproduced with permission from Oxford University Press)

2.6 Terrestrial Bubble Detector Research

There has been extensive research into terrestrial applications of bubble detectors for neutron dosimetry. There are many positive features of this technology that make them desirable for use in space.

2.6.1 Neutron Dosimetry with Bubble Detectors

Bubble detectors offer a desired neutron dosimetry solution because of their technological properties. Among other benefits, these devices are lightweight, portable, simplistic in

operation, and have a high sensitivity. These are several reasons why they have been investigated extensively for terrestrial applications. There is also continual research into improving the design of the bubble detector to operate more effectively and in a wider variety of environments.

In 1996, an experiment conducted by d'Erricot et al. published in the Radiation Protection Dosimetry Journal, had an objective to optimize the dose equivalent response with respect to its energy dependence. Initial experiments were conducted to vary the degree of superheat in the bubble detector and the results showed a fairly constant dose equivalent response for varying energies [31]. Subsequent research was carried out by these scientists in two parts, numerical evaluation, and experimental testing. The numerical evaluation was conducted by folding detector fluence response over more than 150 neutron energy distributions from a list of known measured and realistic spectra [31]. Experimental testing was then carried out to validate the numerical results. Several neutron dosimetry comparison exercises were completed in various environments. These environments included benchmark fields, nuclear power plants, spent fuel storage sites, and stray radiation areas. Results for the experiment concluded in an improved bubble detector prototype with a fairly constant dose equivalent response [31]. The drawback was the prototype was only reliable when environmental conditions were not extreme.

Further research has been conducted to test the bubble detector response to neutrons in the range of 10^4 eV to 2.0×10^7 eV. Bamblevski, Surny, and Dudkin in 1996 published their research testing a set of six detectors with thresholds of 10^4 eV, 10^5 eV, 6.0×10^5 eV, 10^6 eV, 2.5×10^6 eV, and 10^7 eV. The research concluded that the response to neutron energies increase after a minimum neutron energy is reached for each of the detectors until 2.0×10^7

eV, where there is a decrease in sensitivity [32]. Figure 8 below shows the response of the BDS to neutrons. The same detector thresholds used in that study are used in this thesis, with the difference being the research in this thesis is set in a space like neutron energy environment.

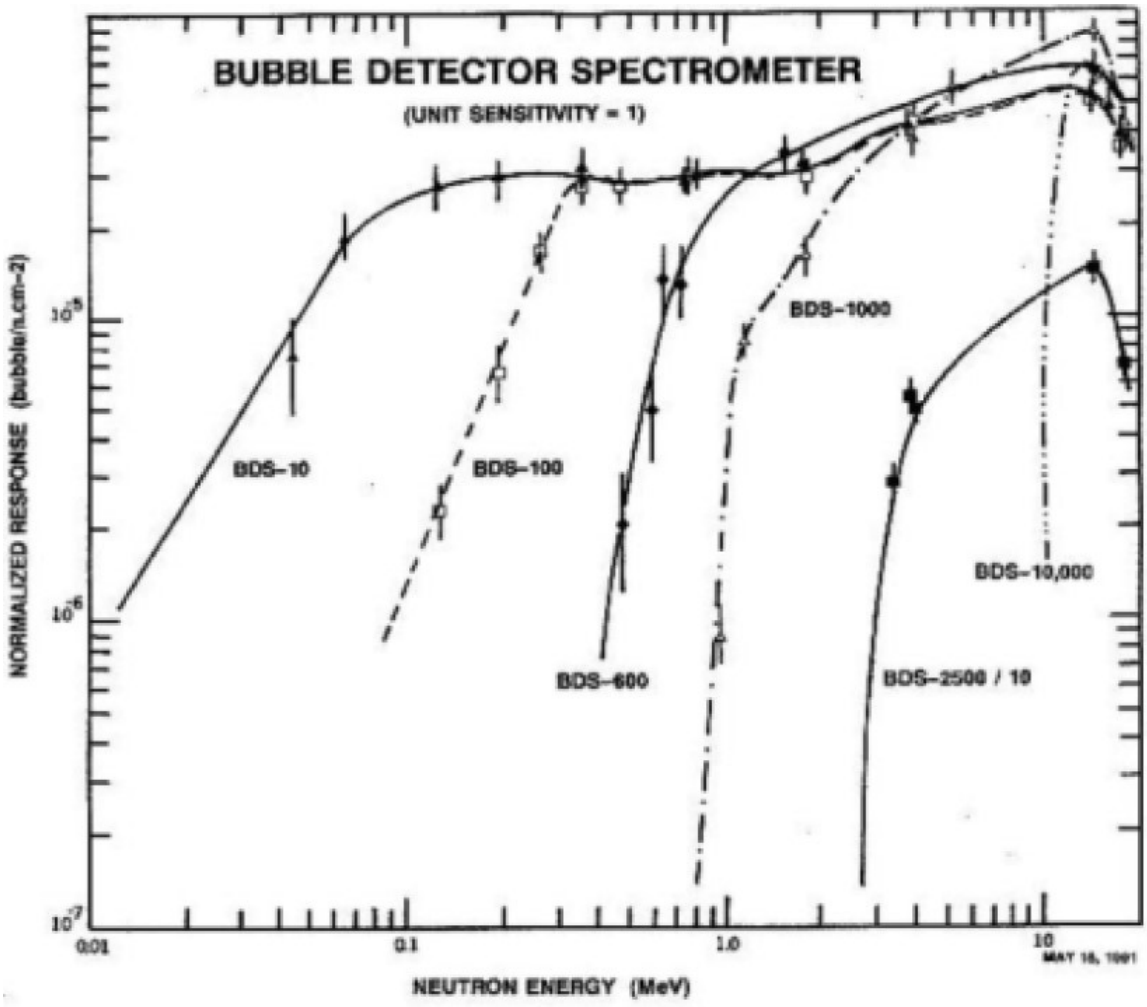

Figure 8: BDS Reponses to Neutrons [32]

(Figure reproduced with permission from Oxford University Press)

2.6.2 Personal Dosimetry with Bubble Detectors

The nuclear industry is expanding into more countries and new technologies. This yields more individuals becoming radiation workers, and therefore personal dosimetry becomes paramount for safety. Bubble detectors are not only used for traditional neutron dosimetry but personal dosimetry as well. In fact, they are the only personal neutron dosimeter with a neutron energy response to meet the ICRP 60 recommendations for a neutron dosimeter [16]. Bubble detectors have many benefits for personal dosimetry such as high neutron sensitivity, a flat energy response, zero sensitivity to gamma radiation, and they can be easily operated [33].

Personal Bubble Detectors (PBD) have been used in the nuclear industry for over 30 years as a reliable dose measurement system. They can be found in a wide variety of applications including nuclear power plants, research facilities, military facilities, and the medical industry. Specifically to the research in this study, bubble detectors are used in space flight and on the ISS.

2.6.3 High-Energy Neutron Dosimetry with Bubble Detectors

Typically, neutron energies of interest on Earth range up to approximately 10^7 eV. However, there are some research activities into high-energy neutron dosimetry using bubble detectors. In one study, the response of superheated drop detectors was investigated in the energy range from 4.9×10^7 eV to 1.33×10^8 eV. The motivation for this study was the growing occupational concerns surrounding high neutron energies at research facilities and during space flight [34]. The experiment was conducted at Universities in Belgium and Sweden, and also at the European Organization for Nuclear Research (CERN) laboratory.

The university methodology utilized neutron energy fields at 4.85×10^7 eV, 6.29×10^7 eV, and 1.37×10^8 eV. These energies were then folded over known fluence responses up to 1.9×10^7 eV. CERN results were analyzed using the HADRON Monte Carlo code. Results from these experiments yielded under-responses from the university experiments of 30-50%, while the CERN study showed an underestimate of ~40% [34].

Studies like these are valuable in improving the safety of workers and the public in the growing nuclear sector exposed to high-energy neutrons. Correcting dose measurements provides more accurate monitoring for research facilities on Earth, and space flights.

2.6.4 Bubble Detector Dose Equivalent Calibration

Bubble detectors from BTI are calibrated using an AmBe neutron field and measurements are taken at different fluences. The AmBe neutron energy spectrum is well known, allowing conversion factors to be developed from experimentation to convert fluence to dose. These bubble detectors from BTI are calibrated using NCRP report 38 [35].

The equivalent dose calibration using AmBe neutrons applies to measurements of fission neutrons because the spectra are similar and bubble detector sensitivity to neutrons in the range of 10^5 eV to 10^7 eV is relatively constant [36].

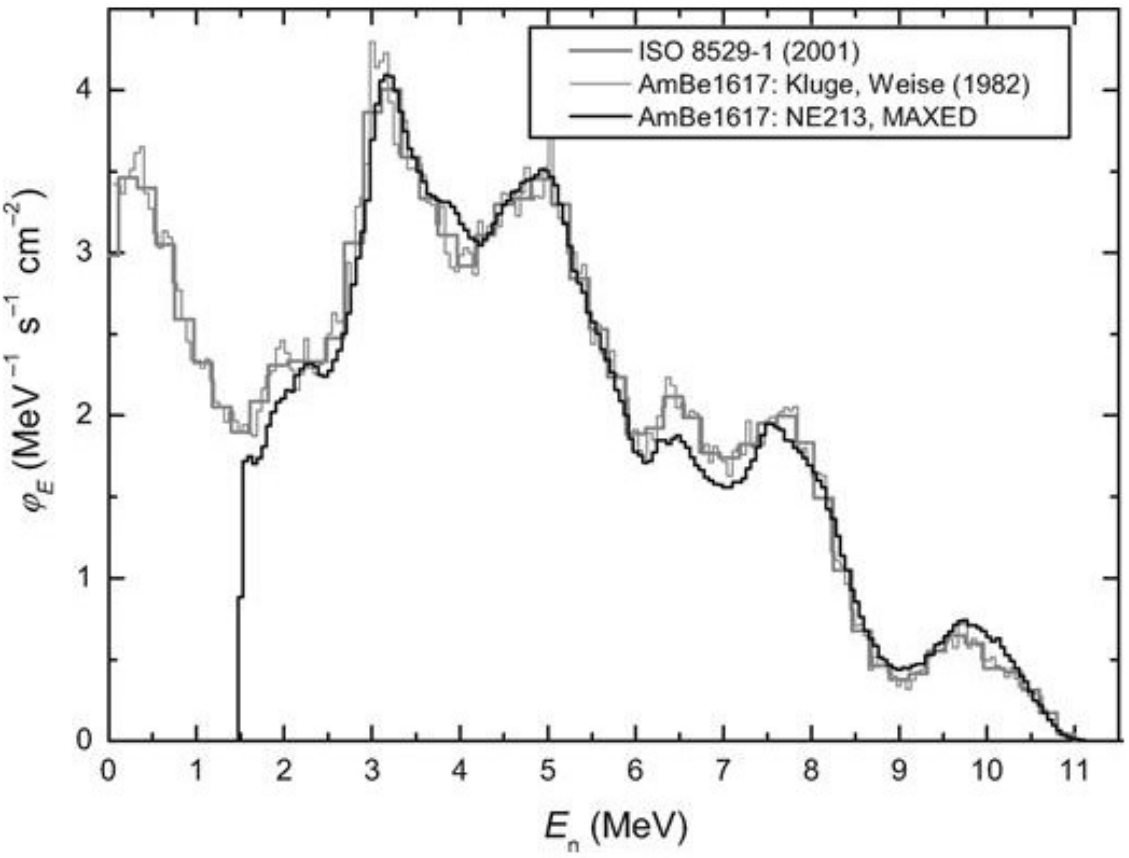

Figure 9: ISO AmBe Neutron Spectrum [37]

(Figure reproduced with permission from Oxford University Press)

2.7 Space Bubble Detector Research

The complex radiation environment on the ISS is made up of photons, heavy charged particles, and neutrons. In the ISS orbit, factors such as the solar activity cycle and orbital parameters play a role in the radiation environment. With this complexity, there have been space studies for dose measured by bubble detectors, but very few have investigated BDS. The various studies reviewed took place during the missions ISS-13 to 15, ISS-16 to 21, and ISS-34 to 37 [38].

2.7.1 Neutron Dose Studies aboard the ISS with Bubble Detectors

A study by R. Machrafi et al between 2008 and 2009 was carried out during space expeditions ISS-13 to 15 to characterize the neutron radiation field on the ISS using SBD's [9]. For the experiment, special space-type bubble detectors were produced so that bubble formation was slower than in the bubble detector used in terrestrial measurements. A mini reader was used to count the bubbles automatically, 16 bubble detectors were placed around the ISS in a spherical phantom and the exposure took 5 days of measurement. Bubble detectors were placed inside and outside the phantom to simulate internal and external dose to the human body. This study concluded that the phantom's internal dose was the same as the external dose. With that data correlation, dosimeters on the body are not an overestimation of the dose received to critical organs [9].

Another study conducted in 2012 set out to analyze the BTI bubble detector in space for its applicability and accuracy [38]. This paper provides an overview of the experiments that have been performed for both ground-based and space studies to characterize the response of these detectors to various particle types in low earth orbit and presents results from the various space investigations. The neutron contribution can be up to 30% of the total dose equivalent in LEO, with 40% of those neutrons having energies higher than 1.5×10^7 eV [38]. A comparison of neutron spectrum measurements can be seen in Figure 10.

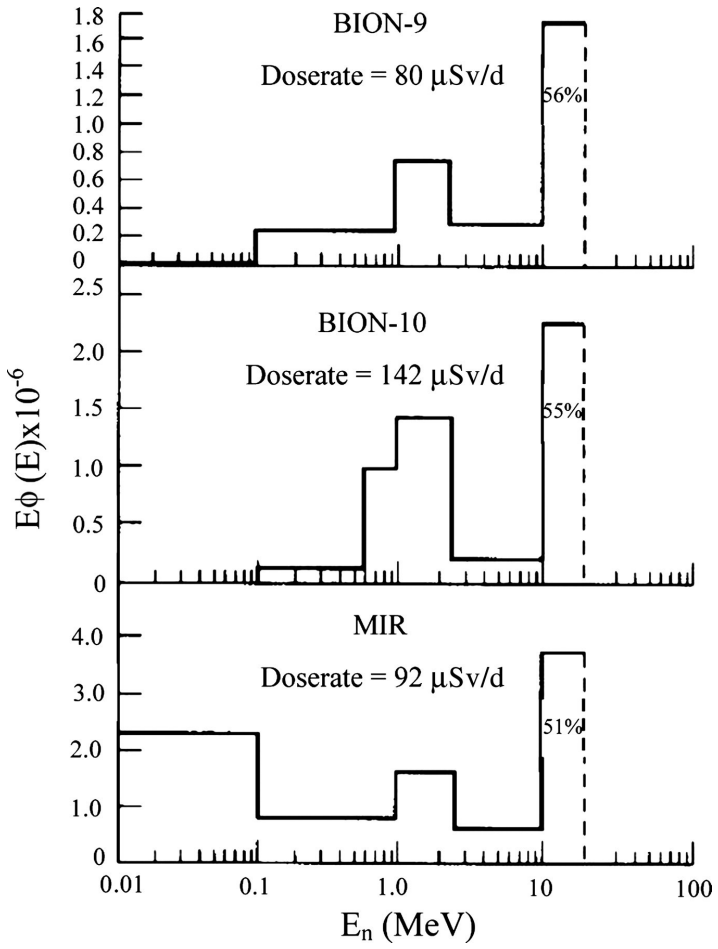

Figure 10: Neutron spectrum measurements from BION-9, -10 and MIR studies [38]

2.7.2 Neutron Energy Spectrum Measurements with Space BDS

Later in 2009, the first measurements using SBDS were conducted to determine the neutron energy spectrum at different locations on the ISS [10]. The SBDS used was similar to the one used in this study, where the energy thresholds of the six bubble detectors used are 10^4 eV (the BDS-10 detector), 10^5 eV (BDS-100), 6.0×10^5 eV (BDS-600), 10^6 eV (BDS-1000),

2.5×10^6 eV (BDS-2500) and 10^7 eV (BDS-10000). Personal neutron dosimeters and SBDS's were used in the study by M. B Smith et al.

The personal dosimeters were calibrated using an AmBe source to determine the detector sensitivities. The temperature and distance from the source to the detector were varied to produce 100-150 bubbles in each detector. For space application, the sensitivity measured using the AmBe source was scaled up by a factor of 1.62 [10], which is based on theoretical calculations and previous ISS dose measurements. For the SBDS, simultaneous measurements were taken with the group of six bubble detectors, and the bubble counts were analyzed using an unfolding technique to evaluate the neutron energy spectrum. A simplified unfolding calculation was used because the statistical significance in some energy bins was low enough to create negative numbers in the formula, which is not physically possible. The results of this study showed that the neutron energy spectrum measured by the SBDS was similar to other measurement techniques. It also concluded that the new SBDS created with a firmer polymer for space application was well suited for dosimetry measurements in that environment [10].

In a subsequent study during space missions ISS-34 to ISS-37 in 2013, more data was obtained for SBDS neutron energy spectrum measurements. Six SBDSs were placed in various locations on the ISS. Similar to the previous experiment, the measurements were unfolded over the response matrix to determine the neutron energy spectrum using the non-negativity constraint. The results showed that the spectrum was similar to previous studies [11].

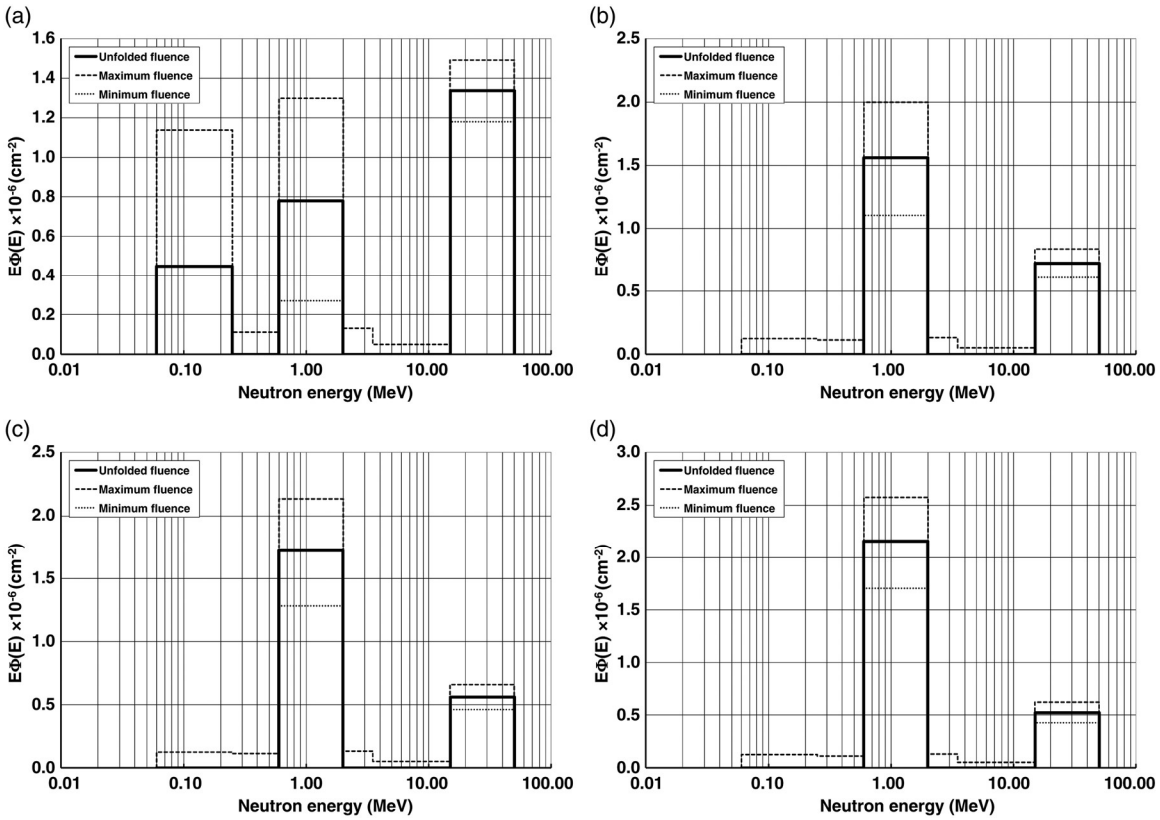

Figure 11: SBDS spectra collected from (a) session A in Columbus, (b) session B in the JEM, (c) session C in US lab, and (d) session D in Node 2 [11]

(Figure reproduced with permission from Oxford University Press)

Chapter 3: Methodology

The experimental investigations in this research were performed using the same BTI SBDS system used onboard the ISS. The BDR-III Bubble Detector Reader from BTI was used to count the number of bubbles created in the SBDS, and all measurements were recorded as shown in the results section of this thesis.

3.1 LANSCE Experiments

The experimental investigation in this thesis was performed using SBDS at LANSCE. The facility has several neutron beam ports with different energies and intensities. In a series of experiments, the Irradiation of Chips and Electronics (ICE House) facility was used. BTI bubble detector measurements were recorded and the number of bubbles counted using the BDR-III Bubble Detector Reader.

The LANSCE facility is located in New Mexico, USA. It is home to one of the most powerful linear accelerators in the world. The exposition of the SBDS to high-energy neutrons was conducted at the LANSCE ICE House facility. ICE House is a neutron beamline from the spallation neutron source with a pulsed 8.0×10^8 MeV proton linear accelerator that is directed to a tungsten target. It produces short bursts of neutrons in an energy range of 6.0×10^5 eV to 7.5×10^8 eV. These resulting neutrons are guided through different beamlines to end-user rooms. The beamlines have been well characterized at the facility and their spectra were measured using a time-of-flight technique. Also, the beamlines range in distance from 10 m to 90 m from the tungsten target at angles of 15^o to 90^o relative to the proton beam direction. For this experiment, the 30L beamline was used since it closely resembles the neutron energy spectrum encountered during space flights.

Neutrons at this beamline travel a distance of 26 m from the tungsten target to the ICE House facility. 30L is the abbreviation indicating the beamline is angled at 30° to the left of the direction of the proton beam. A diagram of the facility is shown in Figure 12 and Figure 13.

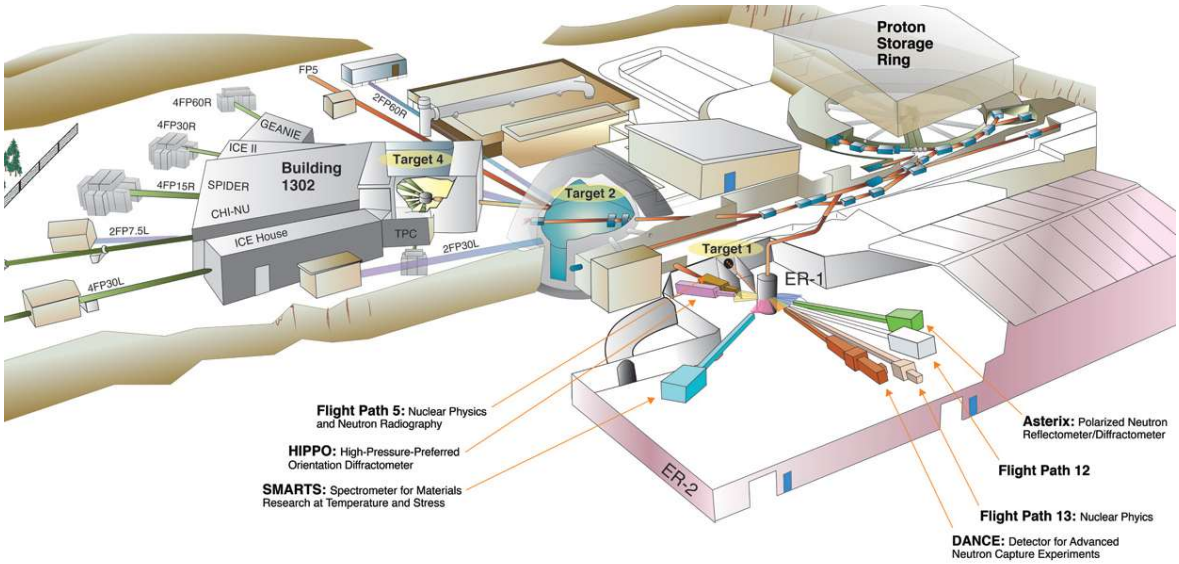

Figure 12: LANSCE Flight Paths and Facilities [39]

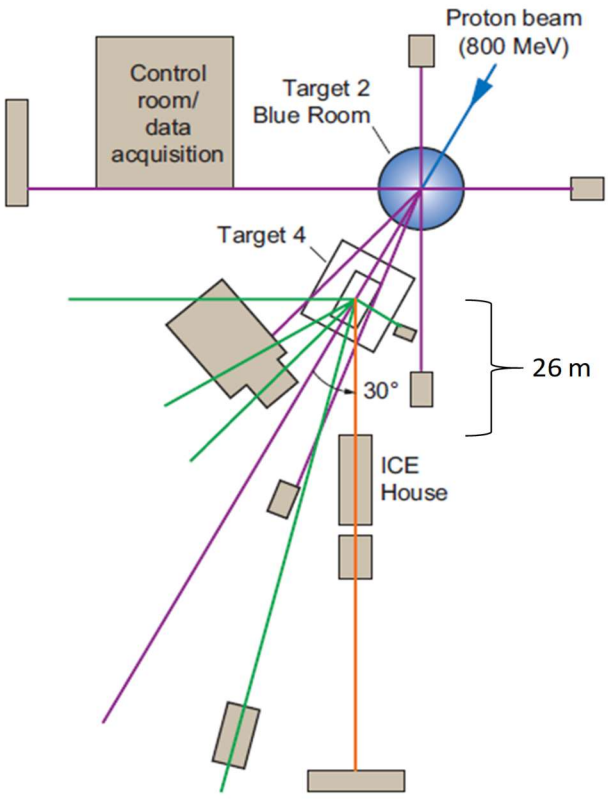

Figure 13: Beamlines at LANSCE

Two SBDS were inserted completely inside the 30L in two separate experiments. Inside the ICE House, the detectors were about 1 m from the beamline entrance. After each irradiation, the number of bubbles was counted using the BDR-III and the corresponding equivalent dose that was measured. The experimental setup showing how the SBDS were exposed is shown in Figure 14. The neutron spectrum generated per pulse from the source is presented in Figure 15.

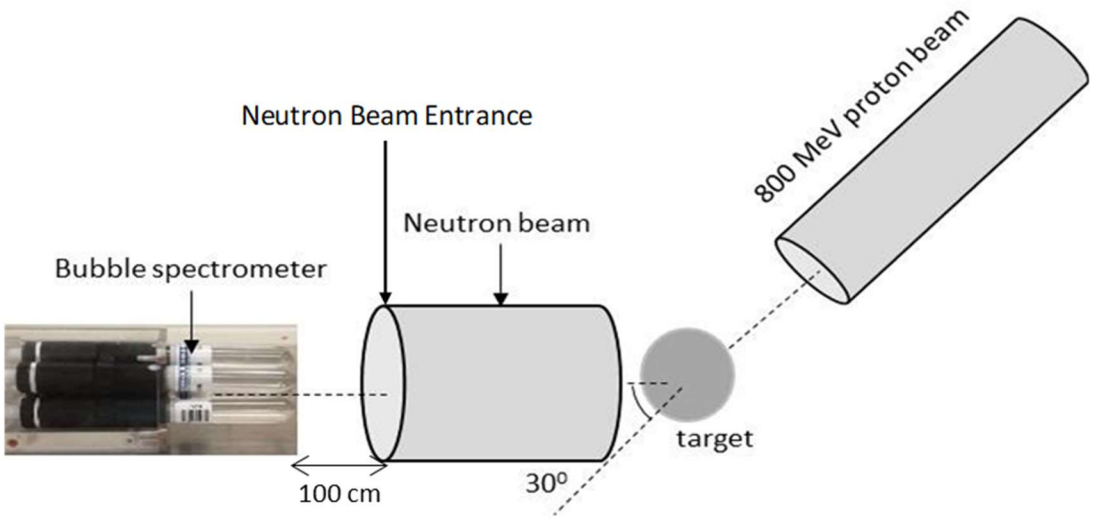

Figure 14: Experimental Setup with the Bubble Spectrometer at LANSCE

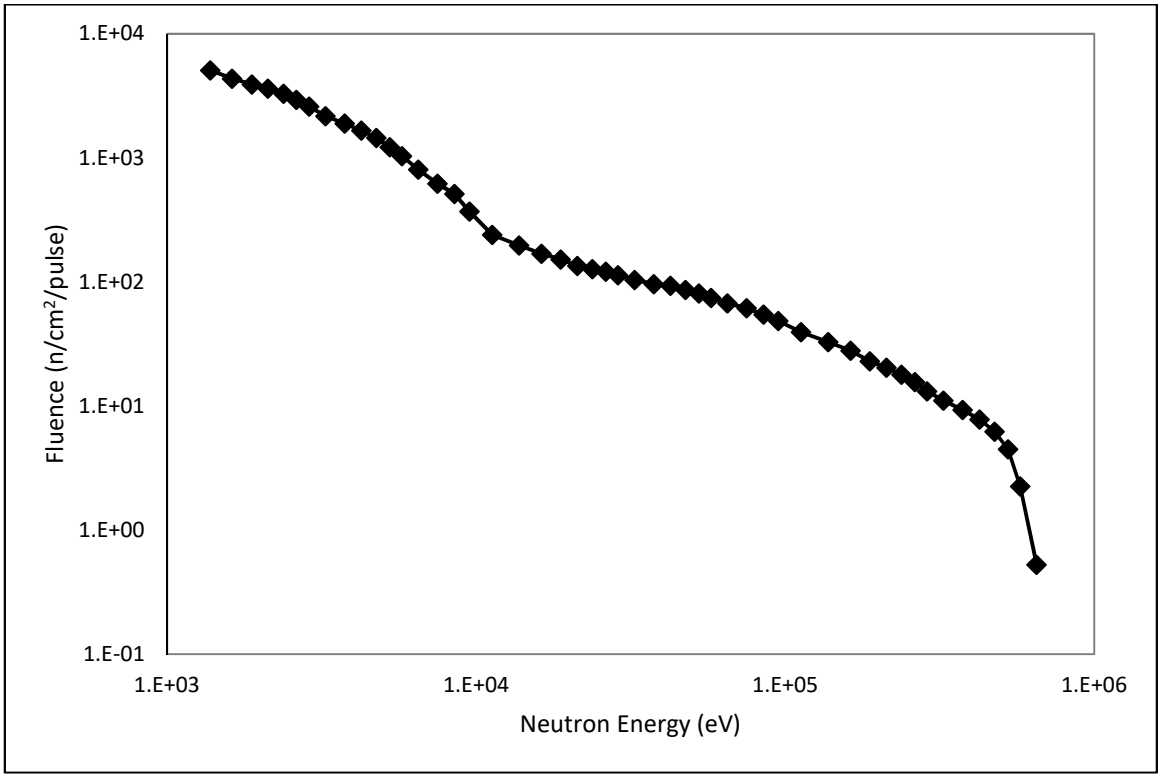

Figure 15: ICE House 30L Beamline Neutron Spectra per Pulse

The neutron spectrum of the ICE House facility is shown in Figure 16 compared to the cosmic ray neutron flux. This cosmic ray spectrum is caused by heavy charged particles interacting with the Earth's atmosphere. The general trend of the flux from LANSCE not identical to the flux experienced on the ISS, but it is sufficiently similar for the energy range of 10^6 eV to 8.0×10^8 MeV. Using the ICE House spectrum provided by the facility, the equivalent dose was obtained by then multiplying by the ICRP74 fluence to equivalent dose conversion factor shown in Figure 4.

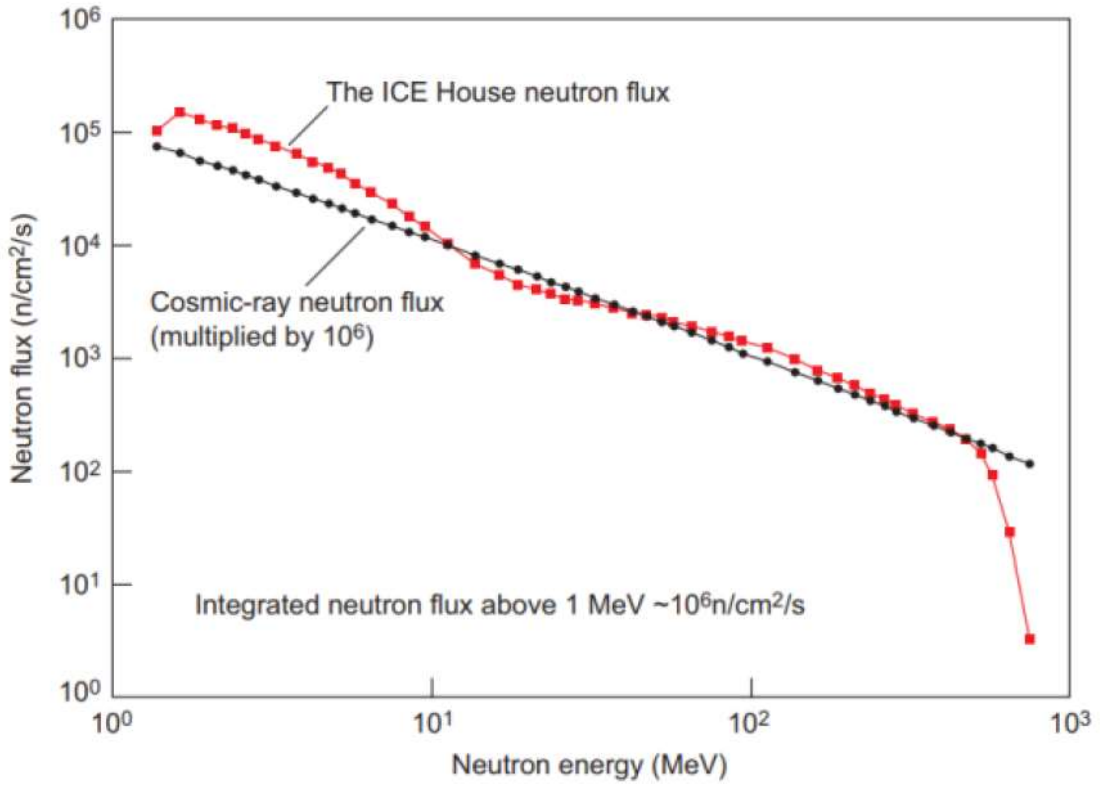

Figure 16: LANSCE Neutron Flux vs Cosmic Ray Neutron Flux [40]

3.2 Space Bubble Detector Spectrometer

The bubble detectors used in this study were Space-Type Bubble Detectors that include two sets of bubble spectrometers and twenty personal bubble detectors. Both devices have a sensitivity comparable to the bubble detectors used aboard the ISS. The detectors were manufactured by BTI. Each detector has a 0.01 L active volume with a total of approximately 10^4 microscopic droplets. For PBDs, the sensitivity ranges from 0.1 – 0.2 bubbles/Sv in an AmBe neutron field. In this type of detector, the polymer is firmer than in commercially available bubble detectors, so the growth of the formed bubbles is slower, allowing the detector to be used for a longer exposure period (generally about 5 days in a space environment). A photograph of a Space Bubble Detector before and after exposure is shown in Figure 17.

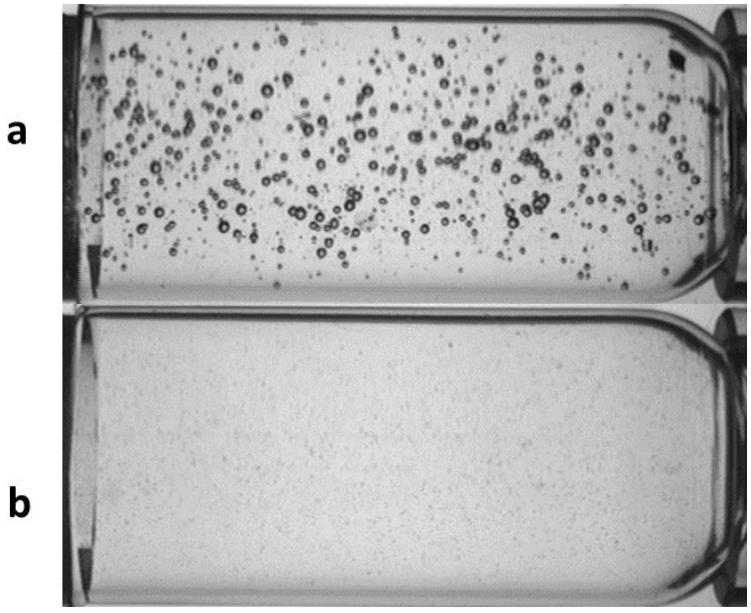

Figure 17: Image of a Space bubble detector (a) after and (b) before exposure to high-energy neutrons

The SBDS consists of six bubble detectors referred to as BDS-10, BDS-100, BDS-600, BDS-1000, BDS-2500, and BDS-10000. The six detectors have a neutron threshold of 10^4 eV, 10^5 eV, 6.0×10^5 eV, 10^6 eV, 2.5×10^6 eV and 10^7 eV, respectively. The spectrometer is not the same as the terrestrial set, but it has a space formulation with temperature compensation applied in the range of 15 – 30°C.

The characteristics of the two SBDS referred to as SBDS1 and SBDS2 used in this current study are listed in Table 1.

Table 1: Characteristics of the Space Bubble Detector Spectrometers

SBDS1		
Detector	**Threshold (eV)**	**Sensitivity (bubbles / Sv)**
BDS-10	10^4	1.90×10^{-3}
BDS-100	10^5	1.20×10^{-3}
BDS-600	6.0×10^5	1.60×10^{-3}
BDS-1000	10^6	1.70×10^{-3}
BDS-2500	2.5×10^6	1.30×10^{-3}
BDS-10000	10^7	0.41×10^{-3}

SBDS2		
Detector	**Threshold (eV)**	**Sensitivity (bubbles / Sv)**
BDS-10	10^4	1.20×10^{-3}
BDS-100	10^5	1.50×10^{-3}
BDS-600	6.0×10^5	1.60×10^{-3}
BDS-1000	10^6	1.80×10^{-3}
BDS-2500	2.5×10^6	2.00×10^{-3}
BDS-10000	10^7	0.39×10^{-3}

For the personal bubble detector exposures, the number of bubbles was counted to extract the dose value using the AmBe detector sensitivity. However, for the bubble spectrometer, bubble counts from the six detectors were unfolded to obtain the neutron dose using the response matrix listed in Table 2. For both PBD and SBDS the neutron dose equivalent was compared to neutron dose equivalent obtained from the neutron spectra along with the fluence to dose conversion coefficients from ICRP74 using the following equation:

$$H_{eq}^{*}(E_n) = \sum_{k=0}^{n} Cf_k(E_n) \times F_k(E_n)$$

Where:

$Cf_k(E_n)$ is the fluence to dose conversion coefficient from ICRP74.

$F_k(E_n)$ is the neutron fluence for the energy bin number k and n is the number of neutron bins.

After exposure, the response matrix is used to determine the neutron energy spectrum. Each bubble detector has a specific sensitivity, which allows the formation of bubbles at that energy threshold or higher. Therefore, to get the proper six bin energy spectrum the detector measurements need to be unfolded. The response matrix used for the SBDS experiments is presented in Table 2.

Table 2: Response matrix of the spectrometer used in the unfolding procedure [38]

#		1	2	3	4	5	6
#	**Detector ID \ MeV**	**0.01 - 0.1**	**0.1 - 0.6**	**0.6 - 1.0**	**1.0 - 2.5**	**2.5 - 10**	**10 - 20**
1	BDS-10	1.25E-05	2.50E-05	2.92E-05	2.97E-05	4.15E-05	4.78E-05
2	BDS-100		2.70E-05	3.14E-05	3.23E-05	4.47E-05	7.20E-05
3	BDS-600			1.90E-05	3.89E-05	5.65E-05	6.48E-05
4	BDS-1000				3.00E-05	4.00E-05	6.85E-05
5	BDS-2500					2.99E-05	8.70E-05
6	BDS-10000						1.20E-04

During the experiment, the SBDS was fully inserted inside the 30L beamline. Images of the set of the bubble spectrometer before the experiment are presented in Figure 18. The specifications from BTI for the SBDS is described in Table 3.

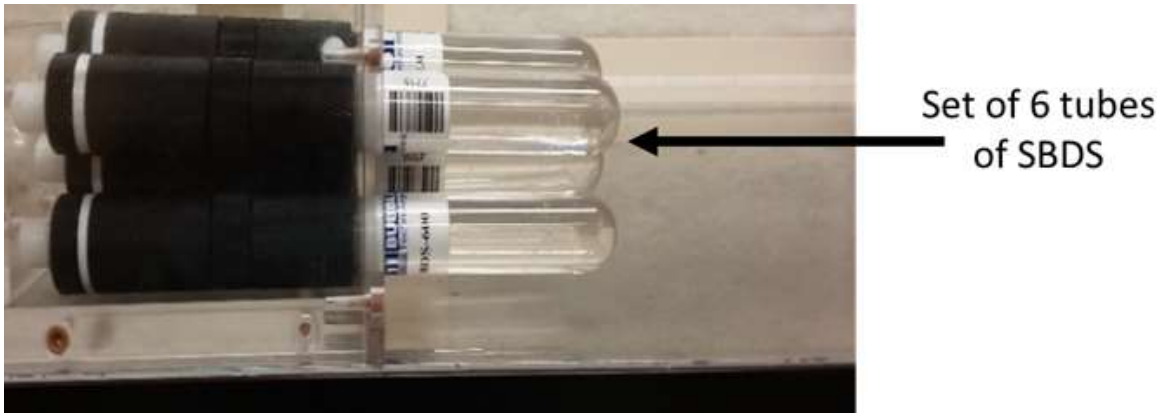

Figure 18: SBDS Experiment Images

Table 3: BDS Specifications [19]

Energy Range:	Six thresholds: 10×10^3, 100×10^3, 600×10^3, 1000×10^3, 2500×10^3, and 10000×10^3 eV
Dose Range:	~ 0.050 rem ~535 Sv
Sensitivity (User Selectable):	0.1 - 0.2 bub/ Sv
Automatic Temperature Compensation:	No
Optimum Temperature Range:	20 °C
Size:	0.08 m length x 0.016 m diameter
Weight:	0.02 kg
Re-Use:	> 10 cycles
Recompression Method:	External recompression chamber required
Notes:	Ideal for neutron spectral characterization
Other:	Zero gamma sensitivity Energy-independent above the threshold, dose rate-independent, tissue equivalent dose measurements Isotropic angular response

3.2.1 Space Bubble Reader

In all experiments, bubble counting was done automatically using a BDR-III Bubble Detector Reader also manufactured by Bubble Technology Industries. The device has been used for all experiments with high-energy neutrons. The BDR-III consists of an optical unit, frame grabber card, and operational software. The reader is shown and all components along with procedures of operation are outlined in the operation manual. A summary of the reader specifications is listed in Table 4.

Table 4: BDR-III Reader Specifications [20]

Size:	0.45 x 0.255 x 0.13 m (17.7 x 10.0 x 5.1 in)
Weight:	5 kg (11 lbs)
Power Supply:	Input: 90-260 VAC, 47-63 Hz, Output: 12 VDC
Camera:	Single 640x480 pixel CCD, 0.0125 m lens
Detector Compatibility:	BD-PND, BDT, BDS
Diagnostics:	Lamp intensity (on start-up) Fluid level (on start-up) USB camera status (on start-up) Detector insertion (in auto mode) Shock cluster (all modes)
Count Time:	< 2 seconds typical (100-150 bubbles)
Count Accuracy:	± 10% for < 150 bubbles
Detector ID:	Manual or barcode entry (optional)
Auto Trigger:	Yes, in automatic mode
Modes:	Manual, Auto, Factory, Calibration (BTI)
Password Protection:	Yes, in Automatic mode
Data Storage:	Grey scale 330k/image, TIFF format Data file MS Access compatible
Required System / Hardware Requirements:	Windows XP/Windows 7/Windows 10 Available USB port

3.2.1 BDS Calibration

Calibration for the SBDS was done by the manufacturer using mono-energetic neutrons at varying energy thresholds. Understanding that each bubble detector in the spectrometer has a unique sensitivity, mono-energetic neutrons of increasing energies were used to calibrate the detector. A typical calibration of the spectrometer was performed using the DRDC-Ottawa Van de Graaff accelerator.

- Mono-energetic neutron beams (4.0×10^4 eV to 1.8×10^7 eV) were used to determine energy thresholds, measure response functions, and test temperature compensation. Data was collected and multiple detectors were irradiated simultaneously.
- A typical experimental setup is shown in Figure 19.

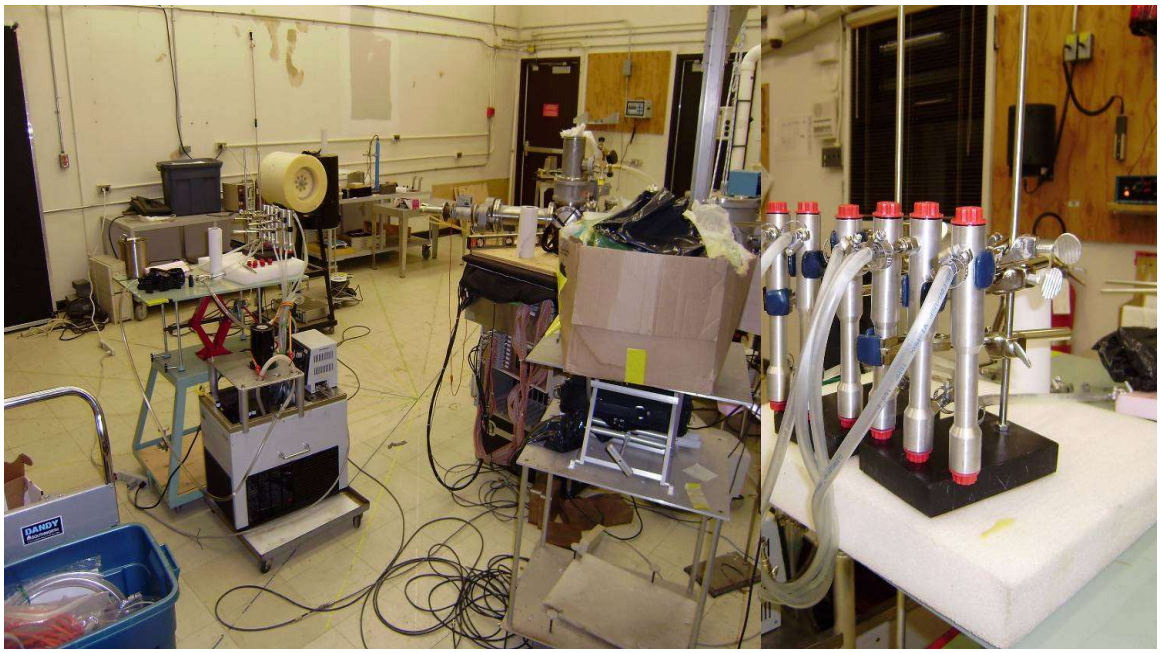

Figure 19: SBDS Calibration Experimental Setup

The calibration began with neutrons of 10^4 eV corresponding to the first spectrometer energy threshold for BDS-10. The following tests were performed:

1. 10^4 eV
2. 10^5 eV
3. 6.0×10^5 eV
4. 10^6 eV
5. 2.5×10^6 eV
6. 10^7 eV

The first test resulted in bubble formation in BDS-10 only. Once that was confirmed, the second test resulted in bubble formation only occurring in BDS-10 and BDS-100. As the neutron energy increased for each step in the calibration, the next bubble detector in the spectrometer showed bubble formation along with the detectors of a lower energy sensitivity. This calibration methodology confirmed that the spectrometer was functioning correctly.

The bubble detector response is calculated by comparing bubble count to fluence measurements performed simultaneously using a long counter (BF_3). The response function was determined using known properties of the nuclear reactions: neutron energy and cross-section as a function of beam energy and angle. The accelerator was operated using different reactions to produce different neutron energies: $^7Li(p,n)^7Be$, $T(p,n)^3He$, $D(d,n)^3He$, and $T(d,n)^4He$. For the BDS-100 detector, high-energy data collected at the iThemba Laboratory for Accelerator-Based Sciences (iThemba LABS, South Africa) in 2007 were also used.

The response data were fitted using the functional form suggested by the PICASSO collaboration [41].

$$P(E, E_{th}) = 1 - \exp a(1 - E/E_{th})$$

Where:

E is the neutron energy,

E_{th} is the threshold energy for the detector,

a is a coefficient.

Parameters E_{th} and a were varied during the fit, along with an amplitude parameter.

The energy thresholds and response matrix were determined from fits to the response data (up to 2.0×10^7 eV), the obtained matrix is for a unit sensitivity (0.001 bubble/rem) detector.

3.2.2 Unfolding Technique

The purpose of the unfolding technique is to extract the neutron spectrum as close as possible to the actual neutron energy spectrum in the environment the detector was irradiated. Accurately calculating the energy spectrum leads to improved dose equivalent calculation. The process evaluates all the fluences for each energy group given a limited number of detector measurements and a corresponding response matrix. Normally, the resolution of the unfolded spectral flux in terms of energy groups is far greater than the number of measurements obtained, which yields an undetermined matrix problem and an infinite number of solutions [42]. The system of equations is defined using the following

equation, where "i" varies from 1 to the number of detectors being irradiated (six in our case):

$$A_i = \sum_{j=1}^{m} \sigma_{ij} * \Phi_j$$

There have been many methods developed to solve the problem, but there is room for improvement. Most solutions are very complex and require a deep understanding of the unfolding technique. These complex mathematical methods also require an initial guess spectrum to solve, called the Priori Spectrum [43]. Due to the potential error inherent in the calculation, the outcome of the neutron fluence can be negative. Since this is physically impossible the accepted methodology is to set that energy bin to zero on account of the non-negativity condition [44].

To determine the neutron energy spectrum measured by the SBDS, and ultimately the total neutron dose equivalent, the SBDS readings must undergo spectral unfolding. This simple calculation converts the BDR-III reading of the number of bubbles into the dose equivalent and is outlined by BTI procedures provided in the manual of the bubble spectrometer.

Starting from the number of bubbles read from the detector, a normalized sensitivity is then obtained by dividing the number of bubbles by the detector sensitivity provided. This is done for each bubble detector in the spectrometer and then the average is taken. From this step, the number of neutrons is then calculated in the corresponding energy range by dividing the unit sensitivity by the response of that bubble detector for each energy interval. The formula is as follows:

$$R_6 = \sigma_{66} * N_6$$

Where:

R is the standardized response for that bubble detector (mrem),

σ is the average response / cross-section (cm^2),

N is the number of neutrons.

Examples of the numbering reference can be found in Appendix C. The next calculation for the number of neutrons would then be as follows:

$$R_5 = (\sigma_{55} \times N_5) + (\sigma_{56} \times N_6)$$

This is procedure repeated until the number of neutrons is determined in each energy interval corresponding to each bubble detector in the spectrometer.

Fluence per MeV is then derived in each histogram by dividing the number of neutrons by the energy range each detector covers. This is then multiplied by the conversion factor to obtain the equivalent dose in each histogram. Finally, the sum of all dose equivalents is taken to determine the overall neutron dose equivalent.

Chapter 4: Results and Analysis

4.1 LANSCE Time-Of-Flight Spectrometer Experiments

To have a benchmark for neutron dose equivalent to compare to the SBDS experiments, the LANSCE spallation neutron source was measured using a TOF Spectrometer at the Los Alamos National Laboratory. The 30L beamline was used because it produces a similar neutron spectrum encountered in the space environment. The neutron spectrum for a single pulse using the 30L beamline compared to the cosmic ray neutron flux is shown in Figure 16. This Figure demonstrates that the 30L beamline at LANSCE was selected for its ability to simulate space-like neutron spectra.

The TOF spectrometer works on basic kinematic concepts. To determine the energy of the neutrons, the following equations are considered:

$$E = \frac{1}{2}mv^2$$

$$d = v\,t \qquad \text{----->} \qquad v = \frac{d}{t}$$

To obtain the energy the velocity of the neutrons is required. The time it takes for the resultant neutrons to travel to the detector is measured from when the pulse occurs and the arrival of the group of neutrons at the detector. The distance is a known quantity for the laboratory setup. Neutrons are produced in bursts and detected in groups corresponding to the time elapsing between the generation of a burst and the arrival at the detector. Over this known distance the time of the neutron flight can then be used to calculate the velocity and consequently the energy of the neutron.

The energy of the protons generated from the accelerator is 8.0×10^8 eV. Using a 30-degree angle to simulate neutron energies in space, resultant neutron energies from when the protons interact with the tungsten target is up to 7.5×10^8 eV.

The dose equivalent as a function of the neutron energy measured at LANSCE is shown in Figure 20 for 260 pulses. The neutron energy range in each pulse was from 6.0×10^5 eV to 7.5×10^8 eV. This benchmark was then used to determine if an adjustment factor would be needed to correct the SBDS measurements to a more accurate dose equivalent. To obtain the dose value, the total fluence was multiplied by the probability of each neutron energy bin per pulse. This value was then multiplied by the ICRP74 [24] conversion factor to calculate the dose equivalent at each energy bin, and then finally multiplied by the number of pulses, N, to get the total dose equivalent of each exposition. The sum of all the dose equivalent values from each energy bin yields the total dose equivalent measured:

$$H = \sum_{i=1}^{n} CF_i \times \Phi_i \times N$$

The conversion factors $\pm CF_i$ used are shown in Figure 4. Examining the conversion factors, it can be seen that the larger the neutron energy, the larger the impact on the dose equivalent measurement. The trend for neutron flux experienced in a space-like environment is as neutron energy increases, the respective flux decreases.

The total dose equivalent measured for 260 pulses was 2.78×10^{-3} Sv, and for 285 pulses it was 4.22×10^{-3} Sv. Details on the dose equivalent for the Time-of-Flight Spectrometer can be found in Table 5 for 260 pulses.

Table 5: Neutron Spectra Measured at Los Alamos

E, MeV	Total Dose Equivalent (Sv) 260 pulses
1.62	2.0908E-04
1.88	2.3844E-04
2.12	2.2376E-04
2.38	2.1554E-04
2.62	2.1109E-04
2.88	2.0114E-04
3.25	1.8643E-04
4.25	1.7244E-04
4.75	1.5259E-04
5.25	1.3882E-04
5.75	1.2594E-04
6.50	1.1184E-04
7.50	9.6037E-05
8.50	8.3231E-05
9.50	6.6094E-05
11.25	5.1949E-05
13.75	4.3684E-05
16.25	3.2221E-05
18.75	2.1496E-05
21.25	1.8267E-05
23.75	1.6072E-05
26.25	1.4478E-05
28.75	1.2894E-05
32.50	1.2109E-05
37.50	1.1542E-05
42.50	1.0741E-05
47.50	9.7971E-06
52.50	8.9825E-06
57.50	8.6904E-06
65.00	8.0540E-06
75.00	7.5847E-06
85.00	7.1028E-06
95.00	6.5351E-06
112.50	6.0434E-06
137.50	5.3833E-06
162.50	4.9080E-06
187.50	4.2120E-06
212.50	3.5984E-06
237.50	3.1291E-06

E, MeV	Total Dose Equivalent (Sv) 260 pulses
262.50	2.5954E-06
287.50	2.3089E-06
325.00	2.0257E-06
375.00	1.7718E-06
425.00	1.5132E-06
475.00	1.3212E-06
525.00	1.1607E-06
575.00	1.0231E-06
650.00	8.5946E-07
750.00	6.5568E-07

Table 6: Neutron Dose Equivalent Measured at Los Alamos

Number of pulses in the Experiment	Los Alamos Dose Equivalent (Sv)
260 pulses	$(2.78 \pm 0.18)\times10^{-3}$
285 pulses	$(4.22 \pm 0.29)\times10^{-3}$

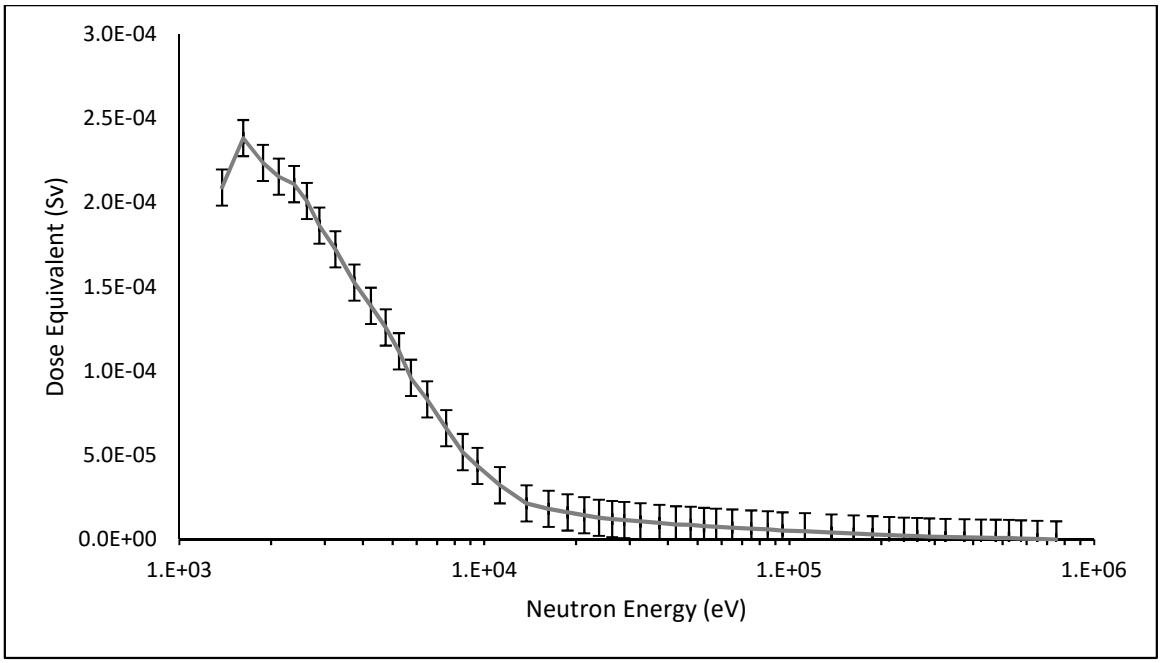

Figure 20: LANSCE Time-of-Flight Spectrometer Neutron Dose Equivalent Result with 260 Pulses

4.2 Space BDS Experiments

As both spectrometers were irradiated, each of the six bubble detectors generates bubbles depending on different energy thresholds. BDS-10 contains bubbles from all energy levels, while BDS-10000 only contains bubbles from neutron energies greater than 10^7 eV. A side by side comparison of each bubble detector in the spectrometer sets is shown in Figure 21 and Figure 22 for SBDS1 and SBDS2, respectively. Examining the bubble reader images, BDS-10000 shows the least number of bubbles. This corresponds to how the spectrometer functions, given that each detector with a lower energy threshold would be counting the bubbles from the higher energy threshold detectors. This also follows the same correlation as the LANSCE neutron energy spectrum shown in Figure 15. The higher the neutron energy, the lower the fluence experienced in space-like conditions.

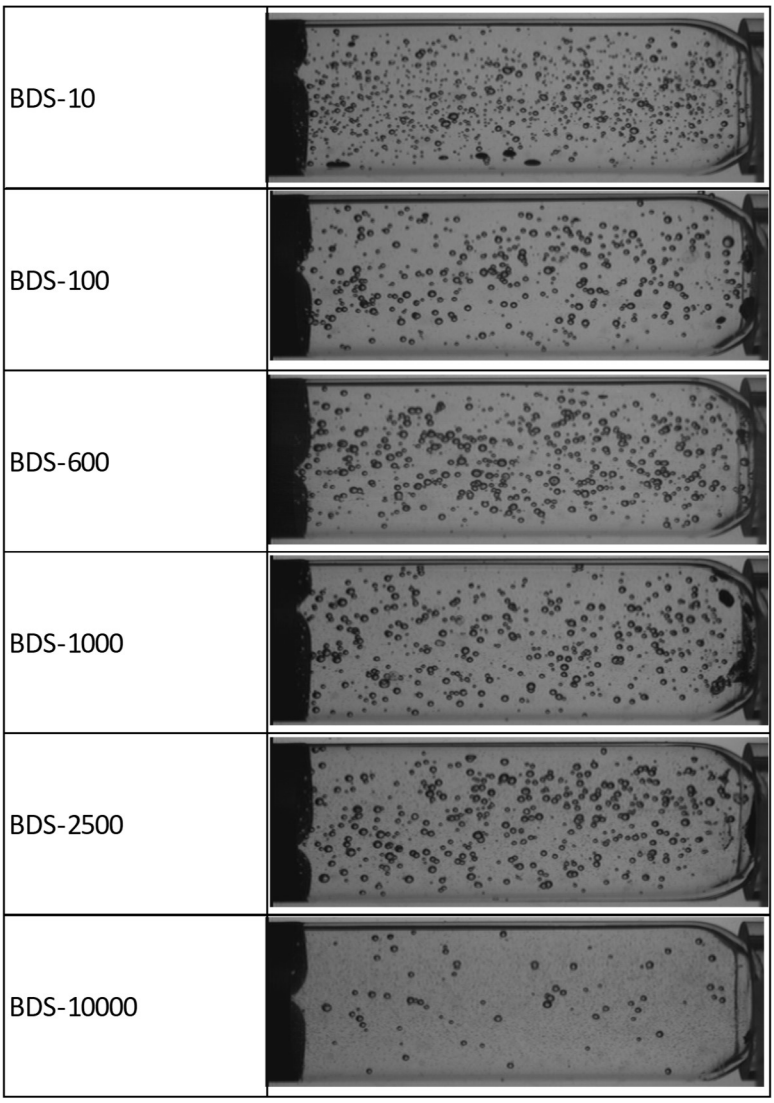

Figure 21: SBDS1 Measurement Images, One-Sided

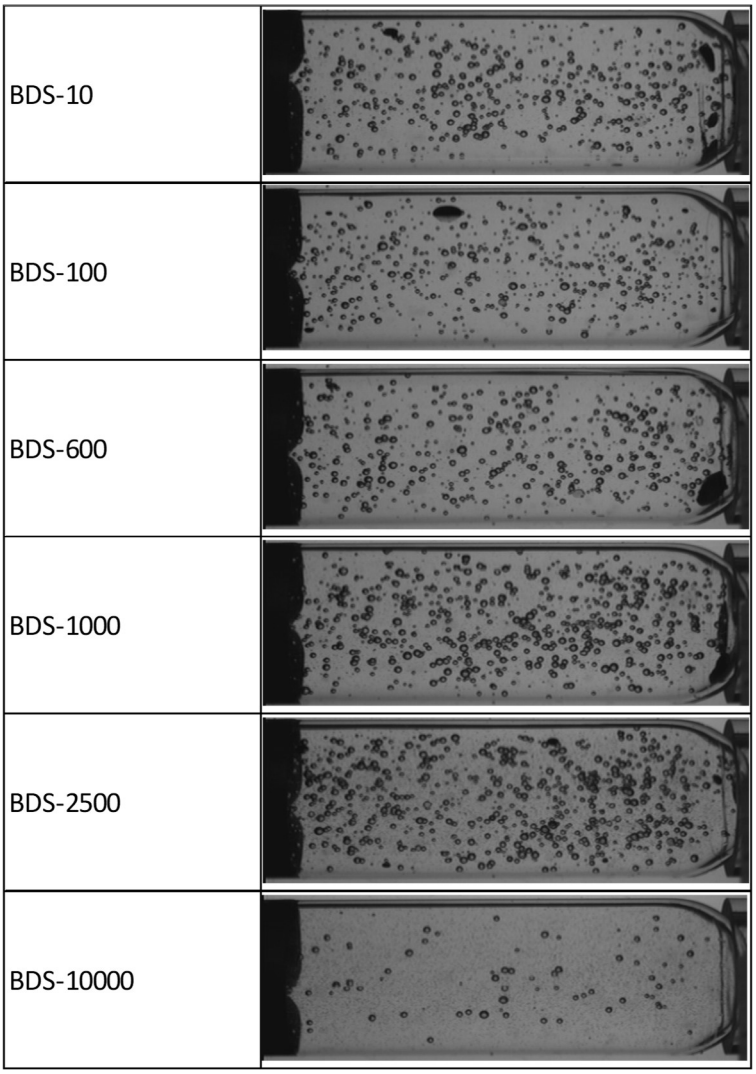

Figure 22: SBDS2 Measurement Images, One-Sided

Unfolding the bubble counts from the bubble detector reader ultimately gives the fluence for each energy bin, determined by the energy threshold sensitivity in each bubble detector. The fluence at each energy interval is shown in Figure 23 for SBDS1. There are six bubble detectors in each spectrometer set, but less than 6 fluence data points. Some fluences were set to zero due to statistical significance because of the non-negativity condition [44] (negative fluence is not physically possible).

For SBDS1, the lowest four energy thresholds were treated using the non-negativity condition. Therefore, only 2.5×10^6 eV and 10^7 eV had an unfolded fluence with any statistical significance. When it comes to calculating the dose equivalent after utilizing the conversion factor, only these two energy bins will have a dose equivalent associated with them. SBDS2 only had one energy threshold that required the non-negative condition, which was 6.0×10^5 eV.

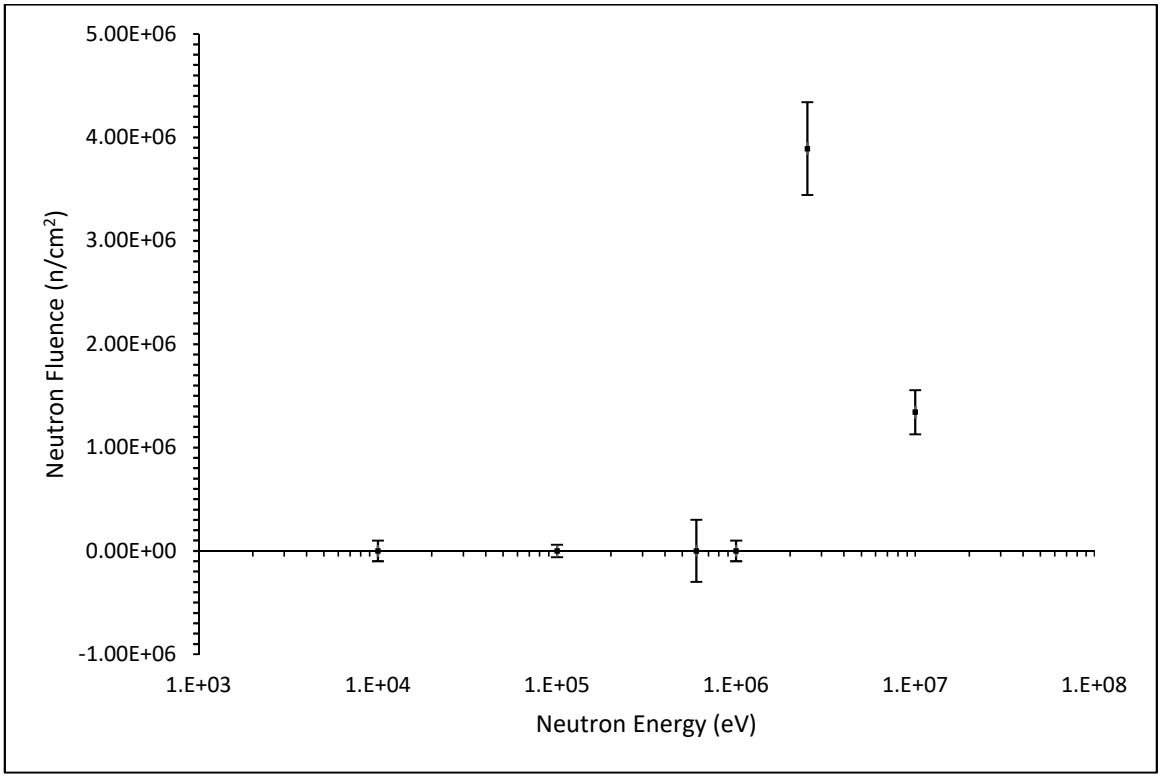

Figure 23: SBDS1 Unfolded Neutron Fluence

These neutron fluence results are similar to those determined in previous experiments. On ISS missions 34-37 from M. B Smith et al, Figure 11 shows SBDS spectra collected from various experiments. It can be seen that the non-negativity condition was required on some

energy thresholds similar to the work conducted in this paper. The other similarity is that there are generally two peaks in the neutron spectra at the 10^6 eV energy bin and the 10^7 eV energy bins. That paper went on to explain that the general features of the unfolded spectra are in agreement with previous measurements of the energy spectrum in space. The expected peaks around 10^6 eV and above 10^7 eV are observed in the data from all four United States Orbital Segment locations. These characteristic features have been observed in earlier work using bubble detectors and other instruments deployed in aircraft and spacecraft [11]. The two neutron energy peaks can also be seen in Figure 10 at the same 10^6 eV and 10^7 eV thresholds [38]. With the same correlation to the previous figure, these results share similar characteristics to the results of this thesis. That study provided an overview of the experiments that were performed for both ground-based and space studies to characterize the response of these detectors to various particle types in low earth orbit.

Using the unfolding technique and applying the non-negativity condition due to statistical significance, the dose equivalent for 260 and 285 pulse can be found in Table 7.

The features of the unfolded dose equivalent spectra are similar to the previous study conducted by Smith et al. [11]. The bubble count from the reader was unfolded using a response matrix with the corresponding cross-sections. For illustration, the output shown in Figure 24 is the dose equivalent in Sv as a function of neutron energy in MeV. The BTI BDR-III has a count accuracy of +/- 10% for bubble counts under 150 [20]. The final dose equivalent was then obtained by taking the sum of the dose equivalent from each energy bin.

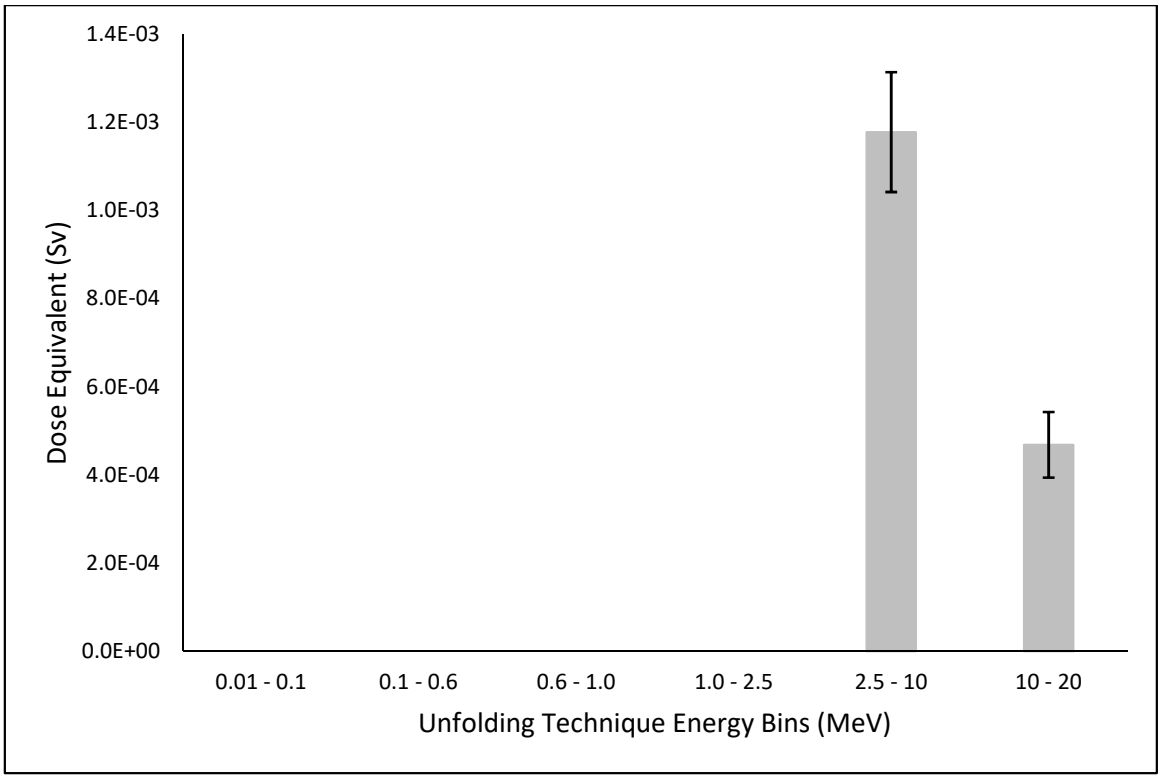

Figure 24: SBDS1 Unfolded Neutron Dose Equivalent Result for 260 pulses

For SBDS1, using 260 pulses, four bubble detectors required their dose equivalents to be corrected to 0 Sv using the non-negative condition. This is because of the statistical error compared to the low bubble count. These detectors were BDS-10, BDS-100, BDS-600, and BDS-1000. The total dose equivalent measured for SBDS1 using 260 pulses was 1.65×10^{-3} Sv. For the second experiment using SDBS2, a similar occurrence happened. BDS-600 required correcting to 0 Sv using the non-negativity condition. All other bubble detectors in this spectrometer resulted in positive dose equivalent values. For SBDS2 using 285 pulses, the total dose equivalent measured was 2.84×10^{-3} Sv.

Comparing the unfolded dose equivalent measurements to the dose obtained from the LANSCE spectra, the adjustment factor found was 1.69 and 1.49 for 260 and 285 pulses, respectively. These ratios were achieved by dividing the LANSCE spectra dose equivalent by the SBDS unfolded dose equivalent.

Table 7: Dose Equivalent Adjustment Factor Ratio

Experiment	#Pulses	Fluence (n/cm^2)	Dose Equivalent (Sv)	Ratio
1 - SBDS1 Unfolding	260	$(1.17 \pm 0.10)\times10^{7}$	$(1.65 \pm 0.21)\times10^{-3}$	1.69
1 - LANSCE Spectra	260	$(1.17 \pm 0.10)\times10^{7}$	$(2.78 \pm 0.18)\times10^{-3}$	
2 - SBDS1 Unfolding	285	$(2.36 \pm 0.11)\times10^{7}$	$(2.84 \pm 0.87)\times10^{-3}$	1.49
2 - LANSCE Spectra	285	$(2.36 \pm 0.11)\times10^{7}$	$(4.22 \pm 0.29)\times10^{-3}$	

It should also be noted that the response function of the SBDS only goes up to 3.0×10^{8} eV, while the space-like neutron energies provided at LANSCE are up to 7.5×10^{8} eV. That difference between the 3.0×10^{8} eV and 7.5×10^{8} eV is the purpose of a calibration factor to ensure readings onboard the ISS from an SBDS is providing reasonable outputs for dose measurements.

Conclusion

As part of the space bubble detector spectrometer ground testing supported by the Canadian Space Agency, the space bubble spectrometer has been exposed to a space-like neutron radiation field using the Los Alamos Neutron facility. In this study, the neutron energy spectra used ranged from 6.0×10^5 eV to 7.5×10^8 eV.

Two experiments with two spectrometers similar to the one used aboard the international space station were conducted. The first one, SBDS1, was exposed to 260 neutron pulses, and the second, SBDS2, was exposed to 285 neutron pulses.

The current use of bubble detectors in space requires an adjustment factor to correct their readings to a more accurate dose equivalent measurement [28].

The obtained results were compared to the neutron dose equivalent measured using the TOF Spectrometer.

This study leads to the following conclusion:

- The dose measured with the bubble detector spectrometer in a space-like neutron field was found to be lower than its value using the ground calibration (response matrix).
- When comparing the LANSCE benchmarked neutron equivalent dose measurements to the space bubble detector spectrometer data, ratios of 1.69 for 260 pulses and 1.49 for 285 pulses were obtained.
- A correction factor of approximately 1.55 should be used to adjust the readings of the bubble detector spectrometer in space neutron spectra.

Future Work

The research presented in this thesis analyzes the SBDS response to neutrons in a space-like neutron radiation field. The obtained results are very specific for the facility used and it is suggested that future work includes evaluating SBDS response in other facilities similar to LANSCE to check the reducibility of the results. Future work would also include the re-evaluation of the readings of the bubble spectrometer aboard the international space station in different locations.

Furthermore, data from the ISS shows that the change in altitude while is LEO imposes no significant increase to the number of bubbles caused by neutrons in a bubble detector. If more studies can prove this to be true, then the BDS would have wide-ranging applications farther than LEO. These could be applied to missions on Mars.

References

[1] H. Ing and A. Mortimer, "Space radiation dosimetry using bubble detectors," *Advances in Space Research,* vol. 14, no. 10, pp. 73-76, 1994.

[2] V. Petrov, "Radiation risk during long-term spaceflight," *Adv. Space Res,* vol. 30, no. 4, pp. 989-994, 2002.

[3] M. Shahmohammadi Beni, T. C. Hau, D. Krstic, D. Nikezic and K. N. Yu, "Monte Carlo studies on neutron interactions in radiobiological experiments," *PLOS ONE,* vol. 12, no. 7, p. e0181281, 2017.

[4] A. Miller, R. Machrafi, E. Benton, H. Kitamura and S. Kodaira, "Comparison of the space bubble detector response to space-like neutron spectra and high energy protons," *Acta Astronautica,* vol. 151, pp. 1-6, 2018.

[5] H. Koshiishia, H. Matsumotoa, A. Chishikib, T. Gokaa and T. Omodakab, "Evaluation of the neutron radiation environment inside the International Space Station based on the Bonner Ball Neutron Detector experiment," *Radiation Measurements,* vol. 42, no. 9, pp. 1510-1520, 2007.

[6] U.-W. Nam, C. H. Lim, J. J. Lee, J. Pyo, B.-K. Moon, D.-H. Lee, Y. Park, H. O. Kim, M. Moon and S. Kim, "Development and Characterization of Tissue Equivalent

Proportional Counter for Radiation Monitoring in International Space Station," *Journal and Astronomy and Space Sciences,* vol. 30, no. 2, pp. 107-112, 2013.

[7] R. M. Ribeiro and D. Souza-Santos, "Comparison of the neutron ambient dose equivalent and ambient absorbed dose calculations with different GEANT4 physics lists," *Radiation Physics and Chemistry,* vol. 139, pp. 179-183, 2017.

[8] M. A. Buckner, R. A. Noulty and T. Cousins, "The Effect of Temperature on the Neutron Energy Thresholds of Bubble Technology Industries‘ Bubble Detector Spectrometer," *Radiation Protection Dosimetry,* vol. 55, no. 1, pp. 23-30, 1994.

[9] R. Machrafi, K. Garrow, H. Ing, M. B. Smith, H. R. Andrews, Y. Akatov, V. Arkhangelsky, I. Chernykh, V. Mitrikas, V. Petrov, V. Shurshakov, L. Tomi, I. Kartsev and L. V, "Neutron dose study with bubble detectors aboard the International Space Station as part of the Matroshka-R experiment," *Radiation Protection Dosimetry,* vol. 133, no. 4, pp. 200-207, 2009.

[10] M. B. Smith, Y. Akatov, H. R. Andrews, V. Arkhangelsky, I. V. Chernykh, H. Ing, N. Khoshooniy, B. J. Lewis, R. Machrafi, I. Nikolaev, R. Y. Romanenko, V. Shurshakov, R. B. Thirsk and L. Tomi, "Measurements of the neutron dose and energy spectrum on the International Space Station during expeditions ISS-16 to ISS-21," *Radiation Protection Dosimetry,* vol. 153, no. 4, pp. 509-533, 2013.

[11] M. B. Smith, S. Khulapko, H. R. Andrews, V. Arkhangelsky, H. Ing, M. R. Koslowksy, B. J. Lewis, R. Machrafi, I. Nikolaev and V. Shurshakov, "Bubble-

detector measurements of neutron radiation in the international space station: ISS-34 to ISS-37," *Radiation Protection Dosimetry,* vol. 168, no. 2, pp. 154-166, 2016.

[12] R. Bedogni, C. Domingo, N. Roberts, D. Thomas, M. Chiti, A. Esposito, M. Garcia, A. Gentile and M. de-San-Pedro, "Invenstigation of the neutron spectrum of americium-beryllium sources," *Nuclear Instruments and Methods in Physics Research,* vol. 763, pp. 547-552, 2014.

[13] United States Nuclear Regulatory Commission, "Basic Health Physics - Neutron Sources," 13 October 2010. [Online]. Available: https://www.nrc.gov. [Accessed 28 April 2019].

[14] J. R. Lamarsh and A. J. Baratta, Introduction to Nuclear Engineering, New Jersey: Prentice-Hall, 2001.

[15] M. F. L'Annunziata, Radioactivity: Introduction and History, from the Quantum to Quarks, Amsterdam: Elsevier, 2016.

[16] G. Zhang, B. Ni, L. Li, P. Lv, W. Tian, Z. Wang, C. Zhang, H. Luo, S. Jiang, P. Wang, D. Huang, C. Liu and C. Xiao, "Study on bubble detectors used as personal neutron dosimeters," *Applied Radiation and Isotopes,* vol. 69, no. 10, pp. 1453-1458, 2011.

[17] J. K. Shultis and R. E. Faw, Radiation Shielding, Manhattan, Kansas: American Nuclear Society Inc., 1996.

[18] R. Sarkar, P. K. Mondal, M. Datta and B. K. Chatterjee, "Note: A new optical method for the detection of bubble nucleation in superheated droplet detector," *Review of Scientific Instruments,* vol. 88, no. 6, 2017.

[19] Bubble Technology Industries, "BDS – BUBBLE DETECTOR SPECTROMETER," 2020. [Online]. Available: http://bubbletech.ca/product/bds/. [Accessed 1 March 2020].

[20] Bubble Technology Industries, "BDR-III – BUBBLE DETECTOR READER III," ForceFive Media, 2020. [Online]. Available: http://bubbletech.ca/. [Accessed 13 February 2020].

[21] J. Shapiro, Radiation Protection, Cambridge Massachusetts: Havard University Press, 1981.

[22] H. H. Barschall, Neutron Sources For Basic Physics and Applications, New York: Pergamon Press, 1983.

[23] ICRP, "Operational Radiation Protection Quantities for External Radiation," *Annals of the ICRP,* vol. 45, pp. 178-187, 2016.

[24] ICRP, "Conversion Coefficients for use in Radiological Protection against External Radiation," *ICRP Publication 74,* vol. 26, no. 3-4, 1996.

[25] A. K. Singh, D. Siingh and R. P. Singh, "Impact of galactic cosmic rays on Earth's atmosphere and human health," *Atmospheric Environment,* vol. 45, no. 23, pp. 3806-3818, 2011.

[26] E. Seedhouse, Space Radiation and Astronaut Safety, Daytona Beach: Springer International Publishing AG, 2018.

[27] L. H. Heilbronna, T. B. Borakb, L. W. Townsend, P.-E. Tsaia, C. A. Burnhama and R. A. McBethb, "Neutron yields and effective doses produced by Galactic Cosmic Ray interactions in shielded environments in space," *Life Sciences in Space Research,* vol. 7, pp. 90-99, 2015.

[28] S. G. Braley, L. W. Townsend, F. A. Cucinotta and L. H. Heilbronn, "Modeling of Secondary Neutron Production," *IEEE Transactions on Nuclear Science,* vol. 49, no. 6, 2002.

[29] J. Bottolier-Depois, M. Siegrist, V. Petrov, V. Shurshakov, V. Bengin and S. Koslova, "TEPC measurements obtained on the Mir space station," *Radiation Measurements,* vol. 35, no. 5, pp. 485-488, 2002.

[30] S. B. Smith, S. Khulapko, H. R. Andrews, V. Arkhangelsky, H. Ing, B. J. Lewis, R. Machraf, I. Nikolaev and V. Shurshakov, "Bubble-Detector Measurements in the Russian Segment of the International Space Station During 2009-12," *Radiation Protection Dosimerty,* vol. 163, no. 1, pp. 1-13, 2015.

[31] F. d'Errico, W. Alberts, E. Dietz, G. Gualdrini, J. Kurkdjian, P. Noccioni and B. Siebert, "Neutron Ambient Dosimetry with Superheated Drop (Bubble) Detectors," *Radiation Protection Dosimetry,* vol. 65, no. 1-4, pp. 397-400, 1996.

[32] V. P. Bamblevski, F. Spurny and V. E. Dudkin, "Neutron Spectrometry with Bubble Damage Neutron Detectors," *Radiation Protection Dosimetry,* vol. 64, no. 4, pp. 309-311, 1996.

[33] D. Ponraju, H. Krishnan, S. Viswanathan and R. Indira, "Preliminary results on bubble detector as personal neutron dosemeter," *Radiation Protection Dosimetry,* vol. 144, no. 1-4, pp. 177-181, 2011.

[34] F. d'Errico, S. Agosteo, A. V. Sannikov and M. Silari, "HIGH-ENERGY NEUTRON DOSIMETRY WITH SUPERHEATED DROP DETECTORS," *Radiation Protection Dosimetry,* vol. 100, no. 1-4, pp. 529-532, 2002.

[35] H. Ing, R. Noulty and T. D. McLean, "Bubble detectors—A maturing technology," *Radiation Measurements,* vol. 27, no. 1, pp. 1-11, 1997.

[36] A. R. Green, B. J. Bennett, B. J. Lewis, P. Tume, H. R. Andrews, R. A. Noulty and H. Ing, "Characterisation of bubble detectors for aircrew and space radiation exposure," *Characterisation of bubble detectors for aircrew an,* vol. 120, no. 1-4, pp. 485-490, 2006.

[37] A. Zimbal, "Measurement of the spectral fluence rate of reference neutron sources with a liquid scintillation detector," *Radiation Protection Dosimetry,* vol. 126, no. 1-4, pp. 413-417, 2007.

[38] B. J. Lewis, M. B. I. H. Smith, R. H. Andrews, R. Machrafi, L. Tomi, T. J. Matthews, L. Veloce, V. Shurshakov, I. Tchernykh and N. Khoshooniy, "Review of bubble detector response characteristics and results from space," *Radiation Protection Dosimetry,* vol. 150, no. 1, pp. 1-21, 2012.

[39] Los Alamos Neutron Science Center, "Facilities," Los Alamos National Laboratory, Jan 2021. [Online]. Available: https://lansce.lanl.gov/facilities/index.php. [Accessed December 2020].

[40] A. Miller, "Investigation of the Bubble Detector Reponse to High LET Space Radiation," University of Ontario Institute of Technology, Oshawa, 2018.

[41] M. Barnabe-Heider and e. al, "The Picasso Experiment," 2007. [Online]. Available: http://www.picassoexperiment.ca/. [Accessed October 2020].

[42] J. Ortiz-Rodríguez and H. Vega-Carrillo, "A Neutron Spectra Unfolding Code Based on Iterative Procedures," IAEA, Mexico, 2012.

[43] B. Mohsin, S. Ahmad, N. Shauka and A. Shaheryar, "Neutron Energy Spectrum Unfolding using Stochastic Techniques," in *International Conference on Power*

Generation Systems and Renewable Energy Technologies (PGSRET) , Pakistan, 2018.

[44] F. d'Errico and M. Matzke, "Neutron spectrometry in mixed fields: superheated drop (bubble) detectors," *Radiation Protection Dosimetry,* vol. 107, no. 1-3, pp. 111-124, 2003.

Appendix A: Bubble Detector Reader Images from the Bubble Spectrometer #1

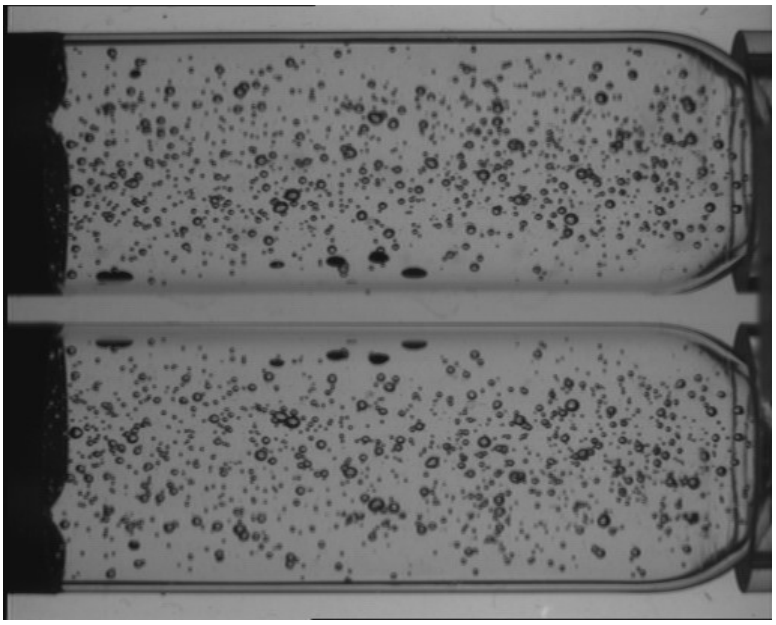

Figure 25: BDS#1 BDS-10

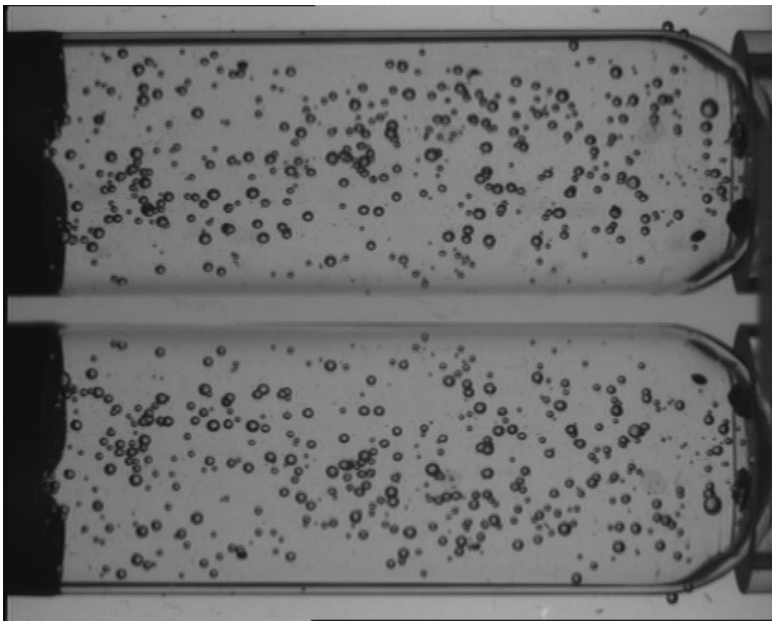

Figure 26: BDS#1 BDS-100

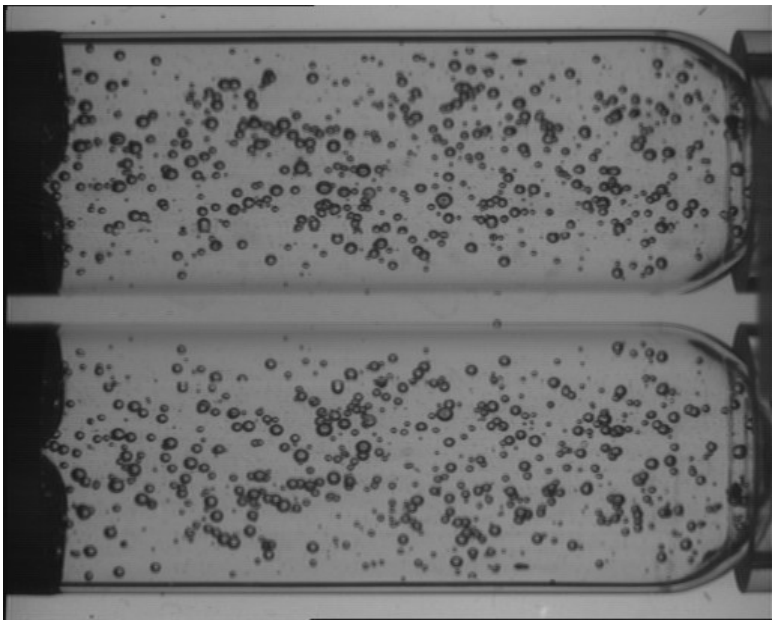

Figure 27: BDS#1 BDS-600

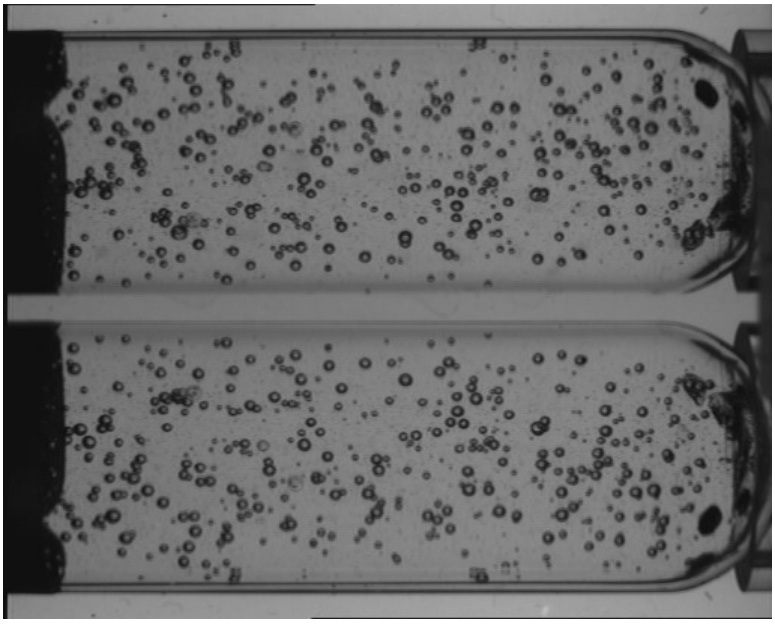

Figure 28: BDS#1 BDS-1000

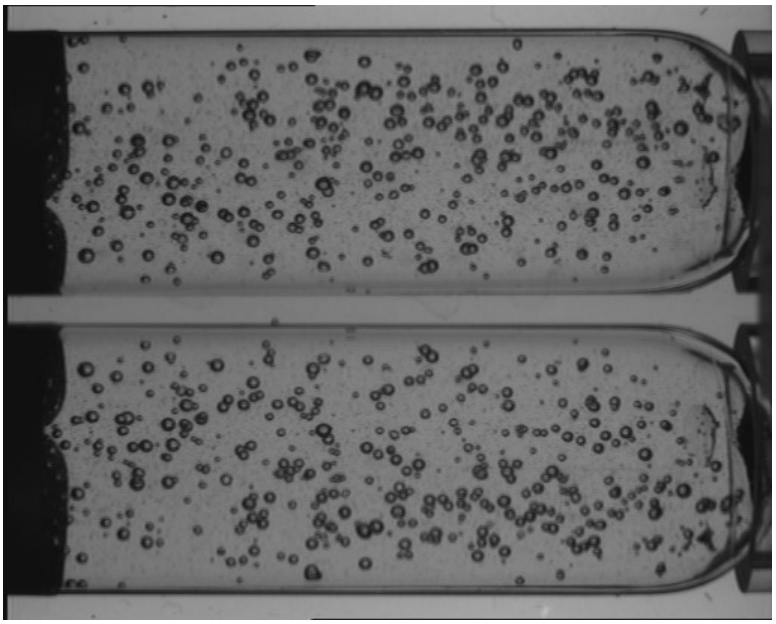

Figure 29: BDS#1 BDS-2500

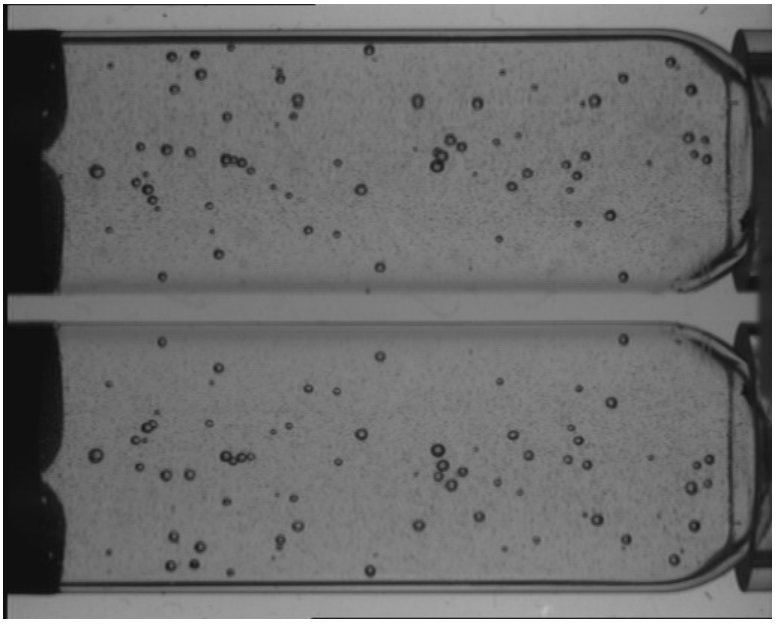

Figure 30: BDS#1 BDS-10000

Appendix B: Bubble Detector Reader Images from the Bubble Spectrometer #2

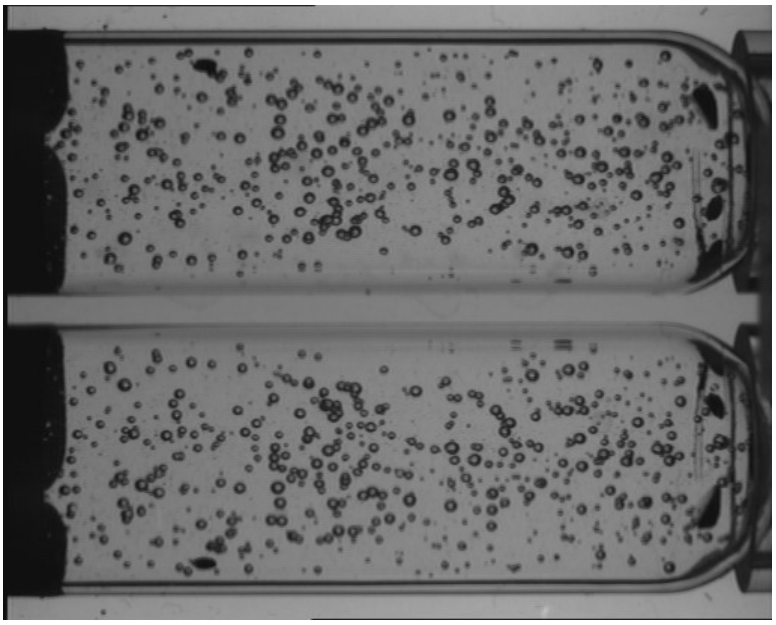

Figure 31: BDS#2 BDS-10

Figure 32: BDS#2 BDS-100

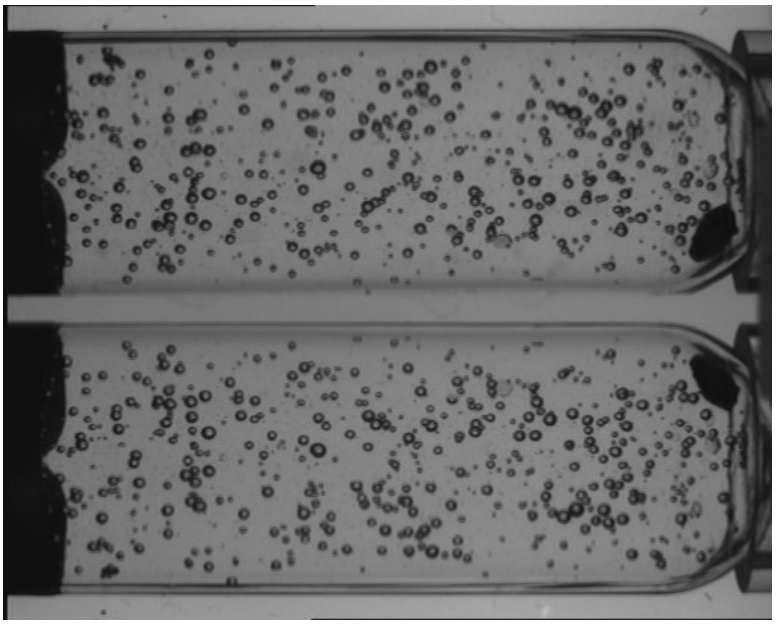

Figure 33: BDS#2 BDS-600

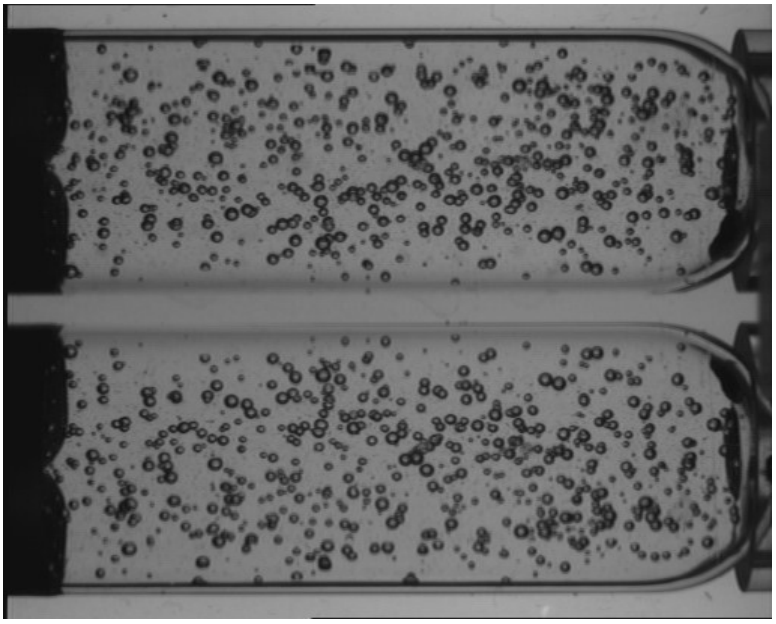

Figure 34: BDS#2 BDS-1000

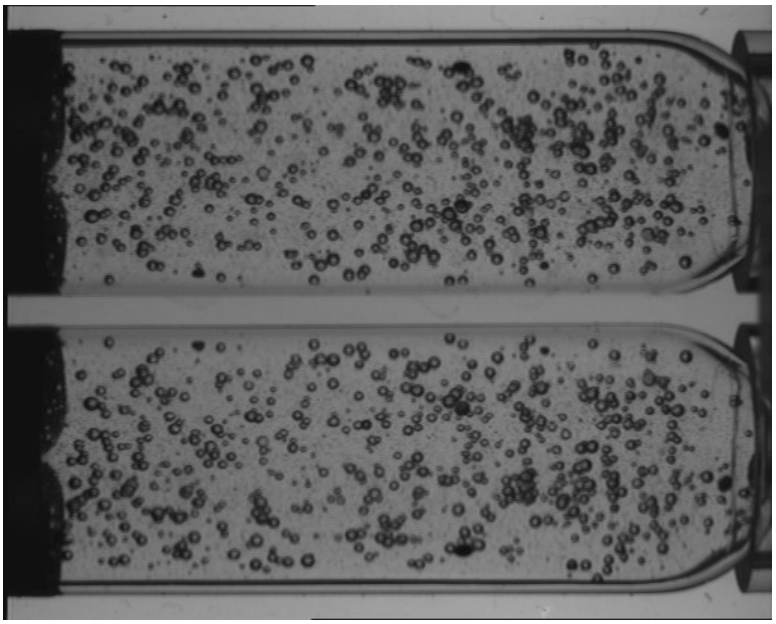

Figure 35: BDS#2 BDS-2500

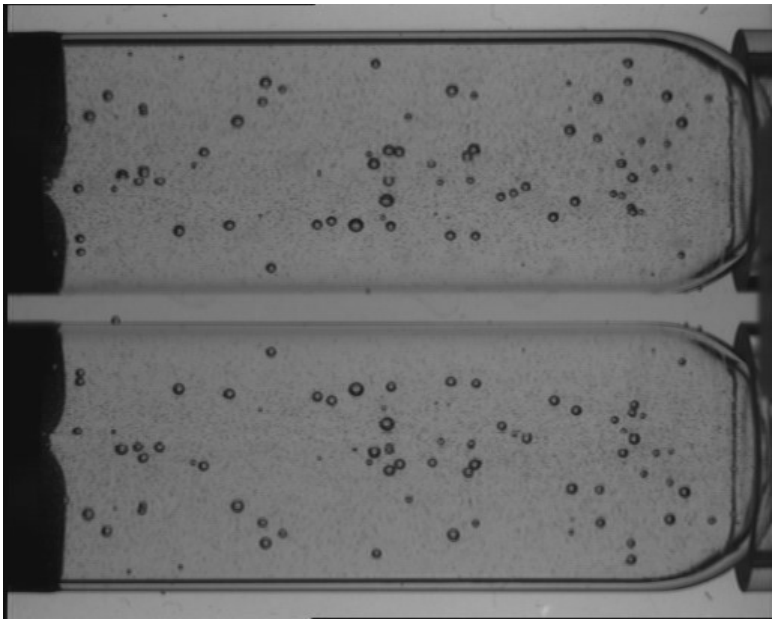

Figure 36: BDS#2 BDS-10000

Appendix C. SBDS1 Unfolding for 260 Pulses

	#	*Bubbles / mrem*	*1*	*2*	*3*	*4*	*5*	*6*
Sensitivity (Written on Bubble Detector)	#	**Detector ID \ MeV**	**0.01 - 0.1**	**0.1 - 0.6**	**0.6 - 1.0**	**1.0 - 2.5**	**2.5 - 10**	**10 - 20**
	1	BDS-10	1.90					
	2	BDS-100		1.20				
	3	BDS-600			1.60			
	4	BDS-1000				1.70		
	5	BDS-2500					1.30	
	6	BDS-10000						0.41

	#	*Ri (mrem) = Ai / Sensitivity*	*1*	*2*	*3*	*4*	*5*	*6*
Standardized Response (Ri)	#	**Detector ID \ MeV**	**0.01 - 0.1**	**0.1 - 0.6**	**0.6 - 1.0**	**1.0 - 2.5**	**2.5 - 10**	**10 - 20**
	1	BDS-10	183.16					
	2	BDS-100		241.67				
	3	BDS-600			200.63			
	4	BDS-1000				168.24		
	5	BDS-2500					233.08	
	6	BDS-10000						160.98

	#	*sigma = cm2*	*1*	*2*	*3*	*4*	*5*	*6*
Average Cross Sections	#	**Detector ID \ MeV**	**0.01 - 0.1**	**0.1 - 0.6**	**0.6 - 1.0**	**1.0 - 2.5**	**2.5 - 10**	**10 - 20**
	1	BDS-10	1.25E-05	2.50E-05	2.92E-05	2.97E-05	4.15E-05	4.78E-05
	2	BDS-100		2.70E-05	3.14E-05	3.23E-05	4.47E-05	7.20E-05
	3	BDS-600			1.90E-05	3.89E-05	5.65E-05	6.48E-05
	4	BDS-1000				3.00E-05	4.00E-05	6.85E-05
	5	BDS-2500					2.99E-05	8.70E-05
	6	BDS-10000						1.20E-04

Appendix E. ICRP74 Conversion Factor

Conversion factor taken from ICRP Publication 74 [24]:

MeV	PSv.cm^2/n (ICRP74)
1.00E-03	3.48
0.01	4.19
0.02	5.72
0.05	10.5
0.1	18.7
0.2	34.8
0.5	77.4
1	126
2	205
3	248
5	294
10	329
14	346
20	367
30	365
50	357
75	373
100	381
150	417
200	432
300	438
500	517
700	627
1000	674
2000	819
3000	903
5000	984
10000	852
20000	1029
50000	1418
100000	1976